INVESTIGATION OF A

QUADRUPOLE ULTRA-HIGH VACUUM ION PUMP

FINAL TECHNICAL REPORT

PERIOD: 1969 through August 31, 1974

REFERENCE: NASA Research Grant
                           NGL 07-009-003 to
                           Rensselaer Polytechnic Institute
                           of Connecticut, Incorporated
                           (now The Hartford Graduate Center)
                           (RPI No. 160.06)·

SUBJECT: Investigation of a Quadrupole Ultra-High
                           Vacuum Ion Pump

Princpal
Investigator: Dr. Helmut J. Schwarz
                           Professor of Physics
                           Rensselaer Polytechnic Institute
                           assigned to The Hartford Graduate Center
                           275 Windsor Street
                           Hartford, Connecticut 06120

                           This report covers the entire period of
                           the Grant which started approximately in
                           March 1969 and ended August 31, 1974.

CONTENTS

PERSONNEL

Besides the principal investigator, the following persons worked at: the research project on a part time basis:

a) Dr. Heinrich Hora, Adjunct Assoc. Professor of Physics, RPI of Conn.

b) Roy C. McCord. Research Associate, RPI of Conn.

c) H.A. Tourtellotte, Senior Laboratory Technician.

ABSTRACT

The new nonmagnetic ion pump resembles the quadrupole ionization gauge. The dimensions are larger, and hyperbolically shaped electrodes replace the four rods. Their surfaces follow $y^2 = 36 + x^2$ (x, y in centimeters). The electrodes, 55 cm long, are positioned lengthwise in a tube. At one end a cathode emits electrons; at the other end a narrowly wound flat spiral of tungsten clad with titanium on cathode potential can be heated for titanium evaporation. Electrons accelerated by a dc potential of the surface electrodes oscillate between the ends on rotational trajectories, if a high frequency potential superimposed on the dc potential is properly adjusted. Pumping speeds (4-100 liter/sec) for different gases at different peak voltages (1000-3000V) at corresponding frequencies (57-100 MHz), and at different pressures (10^{-5}-10^{-9} Torr) were observed The lowest pressure reached was below 10^{-10} Torr.

I   INTRODUCTION

The investigation of a new type of non-magnetic ion pump as per-
formed under this grant originated from a previous NASA grant (NGR
07-009-001) entitled "Study of Non-Magnetic Ionization Gauge with Low
X-Ray Limit" which was also undertaken by the same principal investigator.
The Final Report of that investigation was submitted to NASA Technical
Reports Office, Office of University Affairs, Code Y, Washington, D.C.,
on June 19, 1969. The "Non-Magnetic Ionization Gauge with Low X-Ray
Limit" won the I-R 100 Award of one of the 100 best industrial research
efforts which was presented September 18, 1969, in Chicago, Illinois.

The main objective of this research was to develop and investigate an
ion pump producing, at a high pumping speed, a very low vacuumm in the
order of 10^{-10} torr and lower, which is light weighted and does not need
a magnetic field.

It uses the principle of an electrostatic double quadrupole as it is
sketched in Figure 1. A radio frequency is applied to the four poles
of the quadrupole arrangement so that the electrons will be focused in
the center. At one end there is a hot tungsten wire cathode C, see Fig.
1, and at the other end we have an anticathode which consists of mesh
made of titanium wire or a narrow spiral of titanium wire which can
be heated so that titanium vapor will be available for getter action.
The anticathode is on the same potential as the cathode and a flat ring
which is positioned immediately in front of the cathode. An anode ring
AR is located precisely halfway between cathode and anticathode. It has

a positive dc potential in order to provide acceleration to the
electrons parallel to the tube axis. The quadrupole optics are
properly tuned so that the electrons follow a narrow spiral and
reach their maximum axial velocity when passing through the anode
ring. After this, they are slowed down by the inverted field they
encounter due to the presence of the anticathode. There they turn
back and will have a reverse acceleration. This behavior of the
electrons leads to their oscillation in spiral paths. Therefore,
the free electron path is very long and will only end its free move-
ment when colliding with a gas atom. At very low pressures, for example
10^{-12} torr, it may be as large as 10^{10} cm.

All electrons following these dynamics will have to collide with a gas
atom which in most cases will lead to ionization. The ions produced
will not stay on stable trajectories but will leave the internal part
radially and reach the walls where they might be absorbed and embedded.

II   THEORY OF QUADRUPOLE ION PUMP

The dynamics of the charged particle movement have been investigated
theoretically by many workers; they are described by the Mathieu equations
and their solutions can be found for example, in W. Paul's work on the
mass filter.[1,2] More specifically suited for the devices described here
the principal investigator has given a theory in a paper[3] presented on
invitation at the 4th International Vacuum Congress, Manchester, England
in 1968. This paper, a reprint of which is attached as Exhibit #1, had

been sponsored by the previous NASA grant NGR 07-009-001.

Following this theory a radio frequency is applied to the four electrodes of the quadrupole arrangement so that the electrons will be focused in the center. In the case of ion pumping, we have chosen such parameters that only electrons are being focused.

$$f = 1.03 \times 10^{-10} \; \frac{1}{a} \left(\frac{U_o}{m} \right)^{1/2} \tag{1}$$

where a (see Fig. 2),is the radius of the internal circle; U_o, the maximum voltage of the high frequency generator; and m, the mass of the charged particle. a is given in meters; m, in kilograms; and U_o, in volts so that f comes out in Hertz. For an electron, the above formula would read:

$$f = 1.08 \times 10^5 \; a^{-1} \; U_o^{1/2} \tag{2}$$

For best results the surfaces of the four electrodes should have the shape of hyperbolas.

The theories reported in Refs. 1-5 do not consider space charges. But since with the relatively high ionization yield end electron trapping we cannot anymore neglect space charges, efforts were put into a theory which would at least partly overcome this deficiency. We had successfully tried to obtain a solution considering the space charge of the electrons. It turned out that the mechanism of charge oscillations within the double quadrupole device does not change except for a certain modulation of the

frequency which had been calculated in the case of space-charge-free conditions of the Mathieu equation (see attached reprint of Reference #3).

The particle dynamics in the space-charge double quadrupole device can be expressed by the differential equation:

$$\frac{d^2U}{dx^2} + \eta^2(x) \ U = 0 \tag{3}$$

whereby U is any oscillating quantity like voltage and η the refractive index of the plasma. η is a function of position x and can have a complex value. Equation (3) can be transformed into a Riccati differential equation:

$$\frac{d\psi}{dx} + \psi^2(x) = -\eta^2(x) \tag{4}$$

if $\psi(x)$ is substituted by:

$$\psi(x) \ \frac{d^2U}{dx^2} \ \frac{1}{U} \tag{5}$$

By using a function $v(x)$ being a solution of

$$\eta^2(x) = [v(x)]^2 - \frac{3}{4} \cdot \left(\frac{d}{dx} \ \ell n \ v(x)\right)^2 + \frac{1}{2v} \ \frac{d^2v(x)}{dx^2} \tag{6}$$

We obtain for real $\eta(x)$ a solution of $U(x)$ of Eq.(3):

$$U(x) = \left(\frac{v(0)}{v(x)}\right)^{1/2} \ \exp\left(i \ \int_0^x v(\xi) \ d\xi\right) \tag{7}$$

The solution for U does not show any internal reflection as long as the values of·v(x) exist in accordance with Eq.(6) for a given η(x). The similarity of Eq.(7) with the WBK solution is evident. The main difference is only that in the WBK case a condition of weak·dependence of η on x must exist. The uncertainty of the solutions due to this condition is cancelled in the case of Eq.(7). Restrictions to avoid too strong spatial variations of the refractive index can be derived from Eq.(6); but besides these definite cases, all other solutions are mathematically rigid.

We applied these methods to the equation of oscillation of the particles in a quadrupole system[2-5] as it is used in a quadrupole type ionization gauge. As described in these papers,[2-5] the motion of particles under space charge free conditions is determined by the Mathieu's differential equations

$$d^2/dt^2\ U + (a \pm 2q\ cos2t)\ U = 0 \tag{8}$$

where the double sign distinguishes between the two linear independent solutions. We consider now a differential equation different from Eq.(8) with a few formal changes to fit the conditions expressed in Eqs.(3) to (7). We introduce for the function v

$$v = (a - 2q\ cos2t)^{1/2} \tag{9}$$

The variable x is now the time t. Substituting v(t) from Eq.(9) into the expression for the refractive index, Eq.(6), the differential equation (3) can be modified to:

$$\frac{d^2U(t)}{dt^2} + \left[a - 2q\,\cos2t - 7\left(\frac{q\,\sin2t}{a - 2q\,\cos2t}\right)^2 + \frac{2q\,\cos2t}{a - 2q\,\cos2t} \right] U(t) = 0 \qquad (10)$$

This differential equation has the advantage that without using the detailed knowledge of the Mathieu differential equation, we can exclude non-periodic solutions. These are those where Eq.(6) is singular, e.g. for

$$a < 2q \qquad (11)$$

On the other hand, if

$$q \ll \frac{a}{7} \qquad (12)$$

we can see immediately the oscillating property of U(t):

$$U(t) = \left[\frac{a - 2q\,\cos2t_0}{a - 2q\,\cos2t}\right]^{1/4} \exp(iat)\exp(2iat \mp \cos2t) \qquad (13)$$

U(t) as expressed in the solution of the space charge consideration in Eq.(13) differs from the simple space-charge free quadrupole dynamics by a certain modulation but the basic oscillations remain unchanged.

A physical interpretation of the added terms in Eq.(10) compared with Eq.(8) can be given on the basis of additional potentials created by space charges. Space charges are neglected completely in the analysis of the quadrupole filter[2] which, however, does not affect the insights

on the whole observable mechanism; but the experiments with the quadrupole ionization gauge[3,4] indicate indeed space charge mechanisms, because,there,also lower pressures are involved. The damping mechanism due to the electron-gas and electron-ion interaction, and due to the ionization processes can be discussed formally by a complex parameter η.

III CONSTRUCTION OF QUADRUPOLE ION PUMP - VERSION I

A. Dimensions

The first version was mounted in a stainless steel tube. The four quadrupole electrodes were formed from stainless steel sheets; their surfaces had a hyperbolic shape. The contours followed the equation

$$y^2 = x^2 + 36 \quad \text{(x and y given in cm)} \tag{14}$$

The cross section through the quadrupole tube is sketched in Fig.2.

The electrode surfaces were cut off at a radius R = 11.5 cm. The total length of the electrodes is 55.0 cm. The four hyperbolic surfaces are exactly separated by two ceramic rings at the top and at the bottom. At the top a tungsten spiral serves as anti-cathode; it is covered with titanium which serves two purposes: (1) to act as the anticathode, and (2) to provide titanium vapor for gettering purposes.

Figure 3 depicts a photograph of the hyperbolic electrode structure. The four hyperbolic surfaces are exactly separated by two ceramic rings at the top and at the bottom as can be seen on Fig. 3.

Figure 4 shows a photograph of the quadrupole ion pump version I. . with its hyperbolic electrodes. At the upper end one can notice the tungsten spiral covered with titanium. The whole system was inserted in a large stainless steel container, see Fig.5. As can be seen in Fig.5 a metal system with flanges applying metal seals and bakeable valves was used. Next to the right of the container (see Fig.5) a Redhead Gauge was used for measuring vacua in a range down to 10^{-13} torr. On the same photograph Fig. 5 at the right edge an Ultek Ion pump of 25 liters/sec capacity was connected for comparison. Also a needle valve (black knob at the lower right side of the quadrupole ion pump container) can be seen which allowed bleeding in different gases and obtain a first rough idea of the pumping capacity of the pump under investigation. On the left of Fig.5 are two sorption pumps which provide the proper fore vacuum of about 5μ torr which is necessary to start our ion pump.

B. Electrical Characteristics

The potentials and frequencies applied to the electrodes were adjusted so that the electrons would remain on stable trajectories within the center part of the tube.

According to the theory[1-5] the relationship between peak potential U_o of the high frequency and the dc potential U_{dc} applied to the four electrodes should be:

$$U_{dc} = 0.17 \ U_o \qquad (15)$$

The frequency is then determined by Eq.(2) which for a given geometry is proportionate to the square root of the peak potential U_o.

The potentials and frequencies are listed in Table 1. The electron emission current was adjusted to a stable value i^- with only the dc potential U_{dc} applied to the four hyperbolic surface electrodes. After switching on the high frequency potential with peak potential U_o the emission current i^- decreased to 10% of the initial value.

In operation the quadrupole electrodes carry a potential

$$U = U_{dc} + U_o \cos 2\pi ft \qquad (16)$$

With the cathode and anticathode at a slightly higher positive potential than ground, an ion current i^+ could be measured at the stainless steel housing. The initial electron emission current i^- was usually adjusted to a value of $i^- = 50$ mA.

TABLE I Potentials and frequencies applied to quadrupole ion pump

U_o[volt]	f[MHz]	U_{dc}[volt]
1000	56.87	170
1800	76.30	306
2400	88.00	408
3000	98.40	510

IV   PERFORMANCE CHARACTERISTICS OF VERSION I

Pumping Speed

A paper had been presented at the 5th International Vacuum Congress in Boston, Massachusetts, October 1971 (see Ref.7 and Exhibit #4) on the "Quadrupole Ion Pump Performance Characteristics" of Version I.

As was to be expected from the investigation of the quadrupole ion gauge[4] (Exhibit #2 "Inverse Pressure Dependence of the Quadrupole Ionization Gauge")the pumping speed S increases with decreasing pressure p following a similar anomalous relationship:

$$p^m\ S = a \tag{17}$$

whereby m is much smaller than the corresponding n' in the equation for the quadrupole ion gauge[4] (see Exhibit #2-Table I)

$$i\ p^{n'} = c' \tag{18}$$

namely m = 0.1 compared to n' = $\frac{3}{4}$ being independent of the type of gas to be pumped. However, a in Eq.(17) and c' in Eq.(18) depend on the kind of gas and electrical characteristics (peak voltage U_o, frequency f, ion current i^+).

A more detailed analysis of the measurements of ion current i^+ at different pressures p and varying electrical characteristics leads to

the simple relationship:

$$pS = k(i^+ - i_o^+),$$ (19)

whereby i_o^+, residual ion current at zero pumping speed, follows the quadrupole ion gauge formula

$$p(i_o^+)^n = c$$ (20)

n being the reciprocal value of n' of Eq.(18) and c identical with c'^n as is i identical with i_o^+.

The constant k in Eq.(19) depends solely on the kind of gas used; it has been determined for five different gases - dry air, nitrogen, argon, neon, and hydrogen - and can be taken from Table II. The constant $n = \frac{4}{3}$ in Eq.(20) is independent of the kind of gas; however, c of Eq.(20) behaves similar to the constant a of Eq.(17).

TABLE II Ionization constants for different gases to be applied in Eq. (19)

Gas	k/k_{air}	k[Torr liter sec^{-1} amp^{-1}]
Dry air	1.00	8.35×10^{-2}
Nitrogen	1.00	8.35×10^{-2}
Argon	1.13	9.43×10^{-2}
Neon	0.22	1.84×10^{-2}
Hydrogen	0.44	3.67×10^{-2}

A family of curves depicting pumping speeds at different peak voltages with corresponding frequencies and for the different gases is traced in Figs. 6-8.

Another interesting result is that the relative ionization constant k/k_{air} is equal to the ionization constants as determined in normal ionization gauges. They check with values as measured by others in normal ionization gauges, see for example S. Dushman - J.M. Lafferty, Scientific Foundations of Vacuum Technology, Second Edition, John Wiley and Sons, New York, 1962, pp. 322-323.

The curves of these figures 6-8 follow the empirical equation (19) quite well, but further study will be necessary to explain the physical meaning of the relationship which may be undertaken in the same way as this has been done successfully for the mechanism of the quadrupole ion pump at zero pumping speed, see our publication Exhibit #5, "Theory of the Quadrupole Ion" presented at the 6th International Vacuum Congress, Kyoto, Japan, March 1974. This theory will be a starting point for further investigation of the relationships expressed in Eqs. (17), (19), and (20).

CONSTRUCTION OF QUADRUPOLE ION PUMP VERSION II

In order to further increase the pumping speed it was suggested during a discussion meeting with Mr. Paul Yeager of NASA Research Center, Langley Field, that the hyperbolic quadrupole electrodes should be replaced by mesh type electrodes without affecting the rigidity of the structure which should

have a position accuracy of at least one per mil, as the electron. optics of the system are quite sensitive to deviations from the geometry. The radial throughput of Version I is about 17%. Stainless steel grid type electrodes were produced which had a square mesh structure formed by 1/16" diameter wires 5/16" apart, so that the radial throughput increased to approximately 85%

The modified quadrupole pump Version II is depicted in the photographs of Figs. 9 and 10.

Although the radial throughput of Version II is 5 times as large as that of Version I, the pumping speed did not increase in proportion. Several of the pumping speed measurements as represented by the curves in Figs. 6-8 were repeated. The pumping speeds determined were in all cases about twice as large as those achieved with Version I.

INTERPRETATION ATTEMPT OF RESULTS

A. Observation of Plasma

In order to account for the relationship (18) one had to assume a low density central plasma having the shape of an ellipsoid (see Fig. 11) which does not change its length but only its diameter when varying the pressure, see Ref. 8 (Exhibit #5) p. 7]. It was tried to photograph the plasma, but this was impossible since the background light of the 2500 K hot tungsten filament was obviously brighter than the visible plasma radiation. Filter techniques were necessary. A theoretical analysis

was undertaken assuming that the plasma consisted of hydrogen and that the H_α line of 6563 Å would be bright enough to become observable if a filter would be used to cut off the spectrum of the filament light below and above this wave length.

Naturally it is necessary that the radiation of the plasma must be of higher intensity than that which is emitted from the hot filament. The radiation emitted from the plasma may be mainly line radiation from the recombination and ionization processes. We have estimated the radiation power E_{po} from the H_α-line which is certainly smaller than the total power E_p of emission from the central plasma

$$E_{po} \leq E_p \tag{21}$$

We have determined the width of the filter necessary to cut down the light emission power E_F of the filament to a value E_{FF} so that it is comparable to the emission power E_{po}, i.e., $E_{FF} \simeq E_{po}$.

Both values E_{po} and E_{FF} have been calculated, considering the most intensive line, H_α, of the hydrogen plasma. First E_{po} was determined.

From the pumping speed measurements (See Figs. 6-8) an ion current of $i^+ = 50$ µa was detected which corresponds to a pair production rate R of:

$$R = i^+/e = 3.13 \times 10^{14} \text{pairs/sec} \tag{22}$$

using the elementary charge $e = 1.6 \times 10^{-19}$ Coulomb and assuming only singly

charged ions. Each ionization may create one photon of energy ε = 1.89eV energy for the H_α -line of frequency ν_α = 4.57 x 10^{14} Hz, so that the total emission power will be

$$E_{po} = R \, \varepsilon \, e = 9.5 \times 10^{-5} \text{ Watt} \tag{23}$$

This is to be compared with the total power of radiation emitted from the filament. The surface of the filament is A $\simeq 10^{-6}$m^2 and its temperature $T_F \simeq$ 2,500 K. This leads to a radiation power according to the Stephan-Boltzmann-law:

$$E_F = \sigma \, T_F^4 \, A = 2.2 \text{ Watt} \tag{24}$$

applying σ = 5.67 x 10^{-8} [Wm^{-2}K^{-4}] which is a value more than four orders of magnitude larger than the radiation power of the plasma E_{po}, Eq.(23), we like to observe. It is therefore mandatory to use a filter of transmission half-width $\Delta\nu$ which we tried to calculate using Planck's formula for the spectral emission density. The flux of radiation within a bandwidth dν leaving a light emitting surface of unit area is given by[9]:

$$F(\nu) \; d\nu = \frac{2\pi\nu^2}{c^2} \; \frac{h\nu}{e^{\frac{h\nu}{kT}}-1} \; d\nu \tag{25}$$

$h = 6.63 \times 10^{-34}$ [J · s], Planck's constant; $k = 1.38 \times 10^{-23}$ [J · K^{-1}], Boltzmann's constant; $c = 3 \times 10^{8}$ [m s^{-1}], speed of light in vacuum; ν[Hz], frequency of radiating light; T[K], temperature of radiating source.

A filter of half-width $\Delta\nu$ would let pass only radiation of power per unit area equal to:

$$E_{FF}/A = \int_{\nu_\alpha - \frac{\Delta\nu}{2}}^{\nu_\alpha + \frac{\Delta\nu}{2}} F(\nu)\, d\nu = \frac{2\pi h}{c^2} \int_{\nu_\alpha - \frac{\Delta\nu}{2}}^{\nu_\alpha + \frac{\Delta\nu}{2}} \frac{\nu^3\, d\nu}{e^{\frac{h\nu}{kT_F}} - 1} \tag{26}$$

We are interested in a value of E_{FF} which is larger or at least equal to E_{po}, in other words E_{FF} in Eq.(26) should be set equal to $E_{po} \simeq 9.5 \times 10^{-5}$ W and the equation:

$$\frac{2\pi h\ A}{c^2} \int_{\nu_\alpha - \frac{\Delta\nu}{2}}^{\nu_\alpha + \frac{\Delta\nu}{2}} \frac{\nu^3 d\nu}{e^{\frac{h\nu}{kT_F}} - 1} \simeq E_{po} \tag{27}$$

should be solved for $\Delta\nu$.

In our case (ν_α = 4.57 x 10^{14}Hz and T_F = 2500K)

$$e^{\frac{h\nu_\alpha}{kT_F}} \simeq 6515 \gg 1 \tag{28}$$

Since the range of integration is closely around ν_α, Eq.(27) can be simplified to:

$$\frac{2\pi h\ A}{c^2} \int_{\nu_\alpha - \frac{\Delta\nu}{2}}^{\nu_\alpha + \frac{\Delta\nu}{2}} \nu^3\ e^{-\frac{h\nu}{kT_F}}\ d\nu \simeq E_{po} \tag{29}$$

introducing as usual $\mu = \frac{h\nu}{kT_F}$ leads to:

$$\frac{6\pi\ A\ k^4\ T_F^4}{c^2\ h^3}\ e^{-\mu_\alpha}(\mu_\alpha^2 + 2\mu_\alpha + 2)\ \Delta\mu \simeq E_{po} \tag{30}$$

We then arrive at a value for

$$\Delta\nu = \frac{kT_F}{h}\ \Delta\mu \simeq \frac{c^2\ h^2\ e^{\mu_\alpha}\ E_{po}}{6\pi\ A\ k^3\ T_F^3\ (\mu_\alpha^2 + 2\mu_\alpha + 2)} \tag{31}$$

Entering with the data for $E_{po} = 9.5 \times 10^{-5}$ W, $A = 10^{-6}m^2$; $T_F = 2500$; and $\nu_\alpha = 4.57 \times 10^{14}$ Hz we obtain:

$$\Delta\nu \simeq 3.3 \times 10^{11} Hz$$

or in terms of wave length

$$\Delta\lambda = c \frac{\Delta\nu}{\nu_\alpha^2} \simeq 5 \text{ Å} \qquad (32)$$

Since there is more light in a hydrogen plasma than just the H_α line a filter of a bandwidth of $\Delta\lambda \simeq 5$Å should be more than adequate to photograph the plasma.

Several pictures were taken at different pressures varying from 10^{-6} down to 10^{-9}torr. At lower pressures it was difficult to determine the diameter with an accuracy better than $\pm$ 0.5 cm, since the boundaries appeared quite fuzzy, but at higher pressures the dimensions of the plasma seemed to be more defined. However, the length did not change noticeably with pressure. The results are presented in Fig. 12 and seem to follow the empirical relationship

$$d = a_o p^{-1/2} \qquad (33)$$

whereby, d, the diameter of the plasma, comes out in cm, if p is entered in torr and the constant $a_o = 2.6 \times 10^{-4}$[cm · torr$^{1/2}$].

B. Theory of Inverse Pressure Dependence

In Ref. 8 Exhibit #5 a theory based on the calibration measurements and the plasma shape measurements has been developed. Its main result lies in Eq.(9) of that paper which predicts an ion current i^+ to be:*

$$i+ = \frac{A_o}{\varepsilon_{e1}^{1/2} + \varepsilon_{e2}^{1/2}} \left[\frac{2}{5} \{ \varepsilon_{e1}^2 + (\varepsilon_{e1}^3 \varepsilon_{e2})^{1/2} + \varepsilon_{e1} \varepsilon_{e2} + (\varepsilon_{e1} \varepsilon_{e2}^3)^{1/2} + \varepsilon_{e2}^2 \} - \right.$$

$$\left. - \frac{2}{3} \varepsilon_{io}(\varepsilon_{e1} + \varepsilon_{e1}^{1/2} \varepsilon_{e2}^{1/2} + \varepsilon_{e2}) \right] \tag{34}$$

leading to the relationship as found empirically in Eqs.(18) and (20), if one assumes that the plasma has the shape of an ellipsoid whose major axis does not change but whose diameter varies according to the experimentally found relationship Eq.(33).

As this can be seen from Exhibit #5 a reasonable electron density could be determined.

* For explanation of symbols see Exhibit #5.

VII SUMMARY AND FUTURE IMPROVEMENTS

A high speed ultra high vacuum ion pump without magnetic field con-
sisting of a double quadrupole assembly tuned for electrons was de-
veloped. Pumping speed increases with decreasing pressure and can
reach for example for neon 100 liters/sec at 10^{-9} torr (see Exhibit #4,
Fig. 3).

The inverse pressure behavior, i.e., higher pumping speeds and higher
ion currents at lower pressures was theoretically explained. Pressures
lower than 10^{-10} torr could be obtained

Higher pumping speeds can be expected from multiple devices whereby
several double quadrupole arrangements could be mounted parallel
within one large tube; the pumping speeds S would most likely add up,
i.e., S_{total} would become somewhat less than nS, n being the number of
double quadrupole systems and S the pumping speed of each individual one.
In mounting such a multiple system, neighboring quadrupoles could "share"
poles..

VIII PATENT

A patent on the Quadrupole Ionization Gauge and Quadrupole Ion Pump was
filed through the Research Corporation, New York, N.Y., with the U.S.
Patent Office on October 27. 1969 and granted under No. 3,665,245, see.
Exhibit #3.

The Research Corporation tries to interest companies to manufacture

the device, but due to the fact that still quite an amount of development work is necessary, no company has entered an agreement yet up to the date of this report.

IX   AWARDS

1.   In 1969 the basic device became subject of an "I-R 100 Award selected by Industrial Research as one of the 100 Most Signigicant New Technical Products of the Year "

2.   In 1970 the quadrupole ionization gauge received a NASA Technology Award.

3.'   In 1972 NASA Invention Award.

X   PRESENTATIONS AT MEETINGS

1.   Invited paper on "Quadrupole Ionization Gauge", co-authored by H.A. Tourtellotte, at the 4th International Vacuum Congress, Manchester, England, April 1968.

2.   Paper "Inverse Pressure Dependence of the Quadrupole Ionization Gauge", presented at the 15th National Vacuum Symposium of the American Vacuum Society, Pittsburgh, Pennsylvania, October 1968.

3.   Presentation on "Quadrupole Ion Pump Performance Characteristics", given at the 5th International Vacuum Congress, Boston, Massachusetts, October 1971.

4.   Presentation on "The Theory of the Quadrupole Ion Pump".
      (co-authored by H. Hora) given at the 6th International Vacuum
      Congress, Kyoto, Japan, March 1974.

XI   PUBLICATIONS

      1.   Exhibit #1
            H. Schwarz, Proc. 4th Internl. Vacuum Congr., Part II, Institute
            of Physics and Physical Society Conference Series No. 6, London,
            1968, pp. 685-689.

      2.   Exhibit #2
            H. Schwarz and H.A. Tourtellotte, J. Vac. Sci. Technol. 6, 260-262,
            (1969).

      3.   Exhibit #4
            H. Schwarz, J. Vac. Sci. Technol. 9, 373-375, (1972).

      4.   Exhibit #5
            H. Hora and H. Schwarz, Japan J. Appl. Phys. Suppl. 2, Pt. 1, 69-72,
            (1974). (Proc. 6th Internl. Vacuum Congr., Kyoto, Japan, 1974.)

      5.   H. Schwarz, "Geometry and Properties of the Plasma in a Quadrupole
            Ion Pump", to be published in J. Vac. Sci. Technol., 1976.

REFERENCES

1.   W. Paul, ZS f. Physik <u>140</u>, 262 (1955).

2.   W. Paul and H. Steinwedel, Z. Naturforsch. <u>8a</u>, 448 (1953); W. Paul and H. Raether, Z. Physik <u>140</u>, 262 (1955).

3.   H. Schwarz, Proc. 4th Internl. Vacuum Congr. Part II, Institute of Physics and Physical Society Conference Series No. 6, London, 1968, pp. 685-689 (Exhibit #1).

4.   H. Schwarz and H.A. Tourtellotte, J. Vac. Sci. and Technol., <u>6</u>, 260 (1969) (Exhibit #2).

5.   H.J. Schwarz, U.S. Patent #3,665,245 issued May 23, 1972, Quadrupole Ionization Gauge (Exhibit #3).

6.   H. Osterberg, J. Opt. Soc. Am. <u>48</u>, 513 (1958)

7.   H. Schwarz, J. Vac. Sci. Technol. <u>9</u>, 373 (1972) (Exhibit #4).

8.   H. Hora and H. Schwarz, Japan. J. Appl. Phys. Suppl. 2, Pt. 1, 69 (1974). (Proc. 6th Internl. Vacuum Congr., Kyoto, Japan 1974.) (Exhibit #5).

9.   See for example, E.U. Condon and H. Odishaw, Handbook of Physics, McGraw-Hill, New York, N.Y. 1958, p. 6-15.

FIGURES

Fig. 1: Schematics of Quadrupole Ion Pump

The positive ring electrode was removed later and the

anode potential superimposed on the quadrupole electrodes.

Fig. 2: Cross Section of Hyperbolic Electrode Surfaces

a = 6cm; R = 11.5 cm $y^2 = a^2 + x^2$ (a = 6)

Fig. 3: Hyperbolic Electrode Structure. a = 6 cm (Version I).

Fig. 4: Quadrupole Ion Pump with Hyperbolic Electrodes and Spiral

Anti-Cathode. Version I.

Fig. 5: Complete Quadrupole Ion Pumping System, Version I. (H.A. Tourtellotte.)

Fig. 6: Pumping Speed as a Function of Pressure at Different Peak

Voltages for Argon. $i^- = 50$ ma. Version I.

Fig. 7: Pumping Speed as a Function of Pressure at Different Peak

Voltages for Hydrogen. $i^- = 50$ ma.

Fig. 8: Pumping Speed as a Function of Pressure at Different Peak

Voltages for Neon. $i^- = 50$ ma.

Fig. 9: Hyperbolic Mesh Wire Electrode Structure. Version II.

Fig. 10: Quadrupole Ion Pump; Version II.

Fig. 11: Schematics of quadrupole ion pump with a stationary centra

ellipsoidal plasma of radius r, in which electrons are con

fined electrodynamically by an RF field.

Fig. 12: Diameter d = 2r of plasma as a Function of Pressure p

$[d = a_0 p^{-1/2}]$.
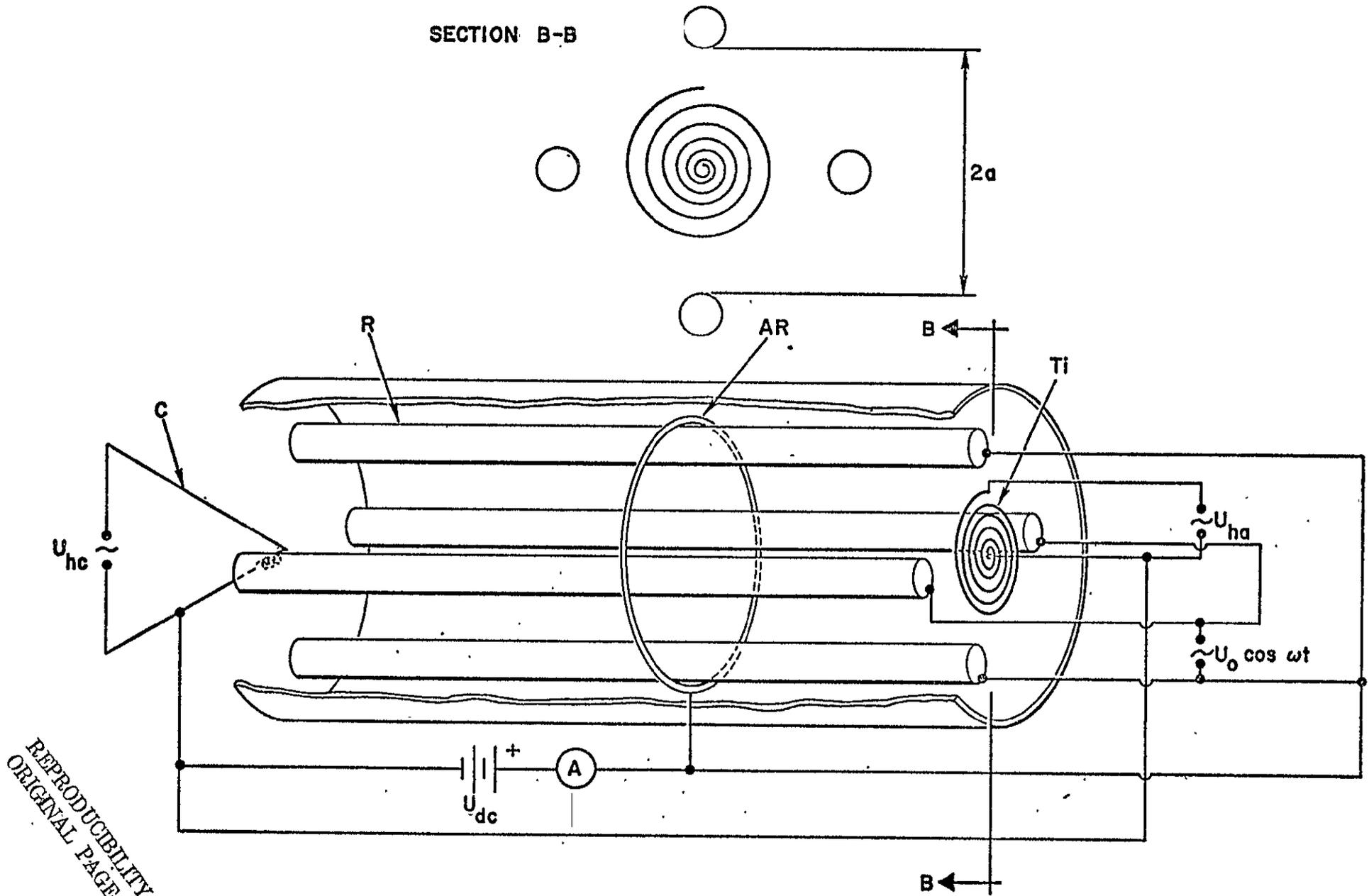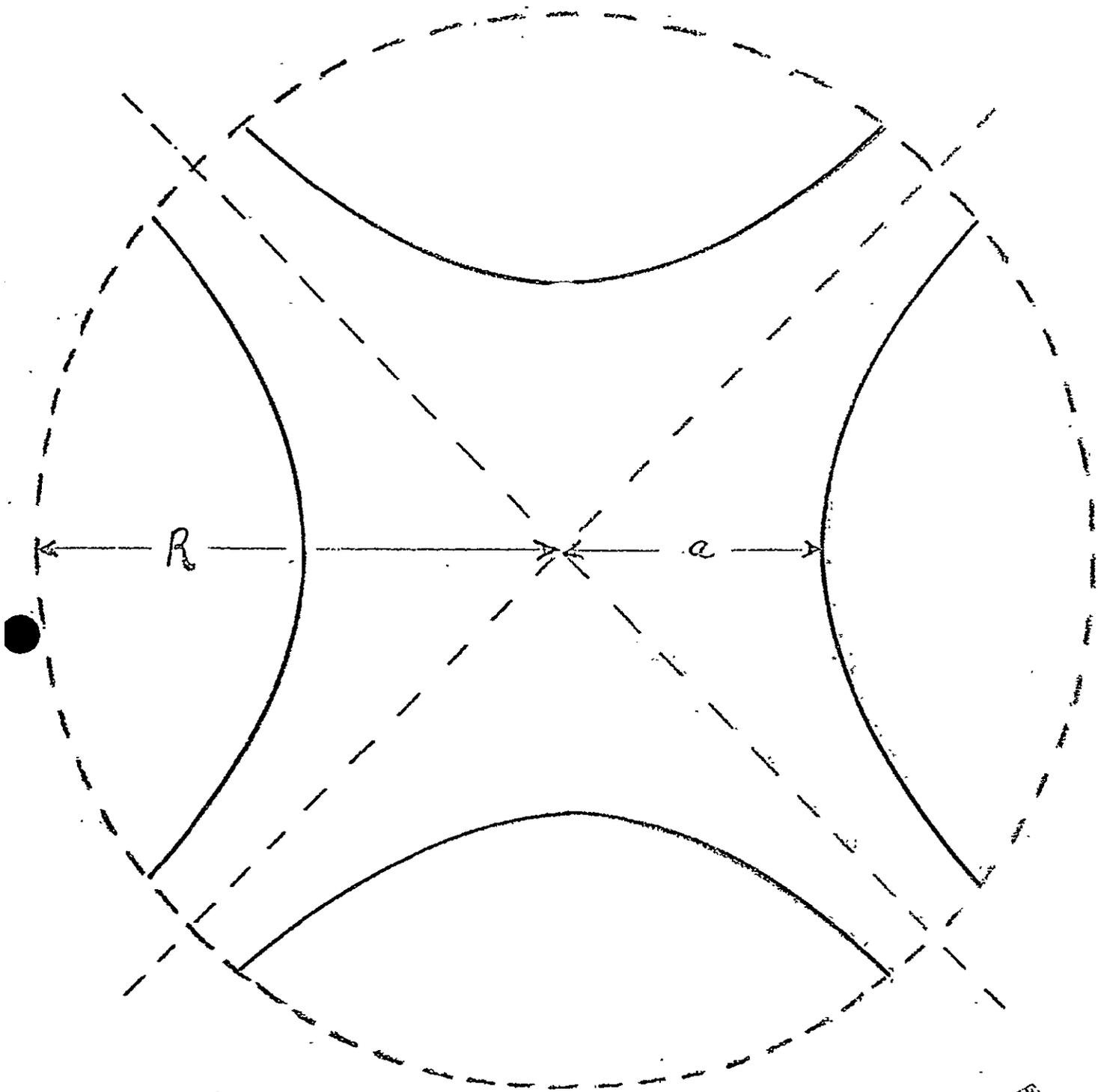
SECTION B-B

$2a$

R

AR

B

Ti

C

$U_{hc} \sim$

$\sim U_{ha}$

$\sim U_0 \cos \omega t$

U_{dc}

A

+

B

Figure 1

Figure 2

FIGURE 3

FIGURE 4

FIGURE 5

Figure 6

Figure 7

Figure 8

FIGURE 9

FIGURE 10

ION COLLECTOR

THERMIONIC EMITTER

END PLATE

CENTRAL PLASMA DIAMETER 2r

ANODE

QUADRUPOLE BARS (4)
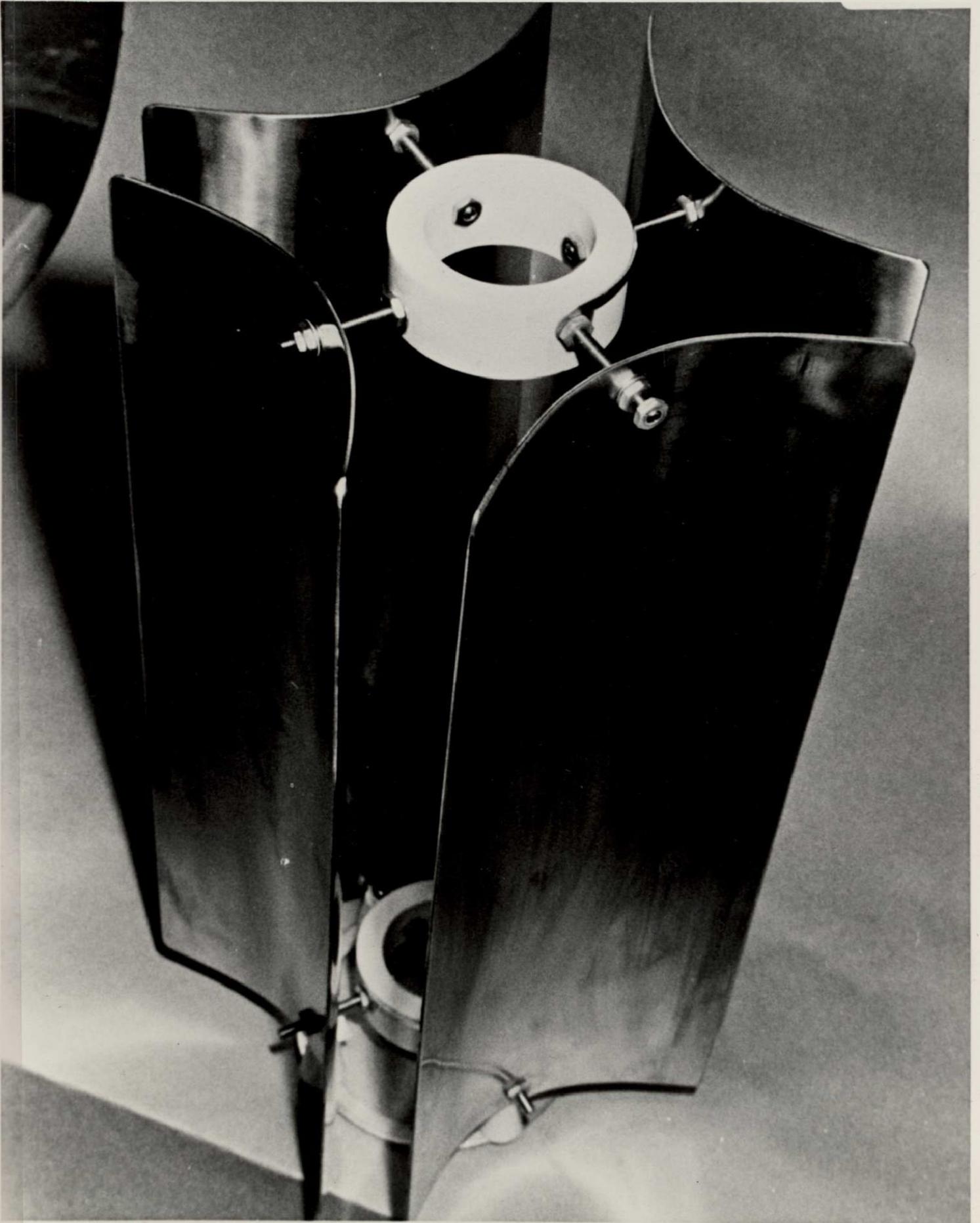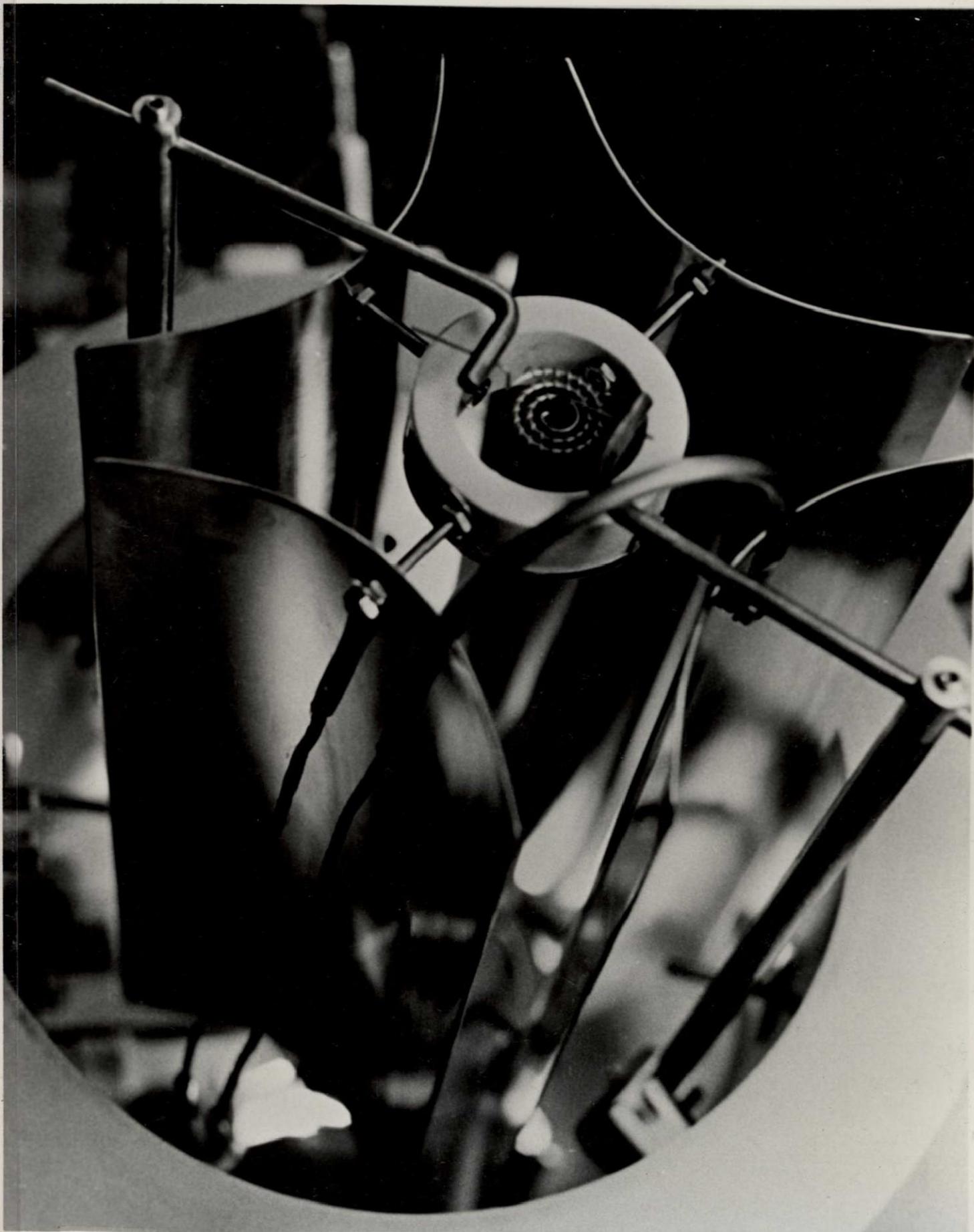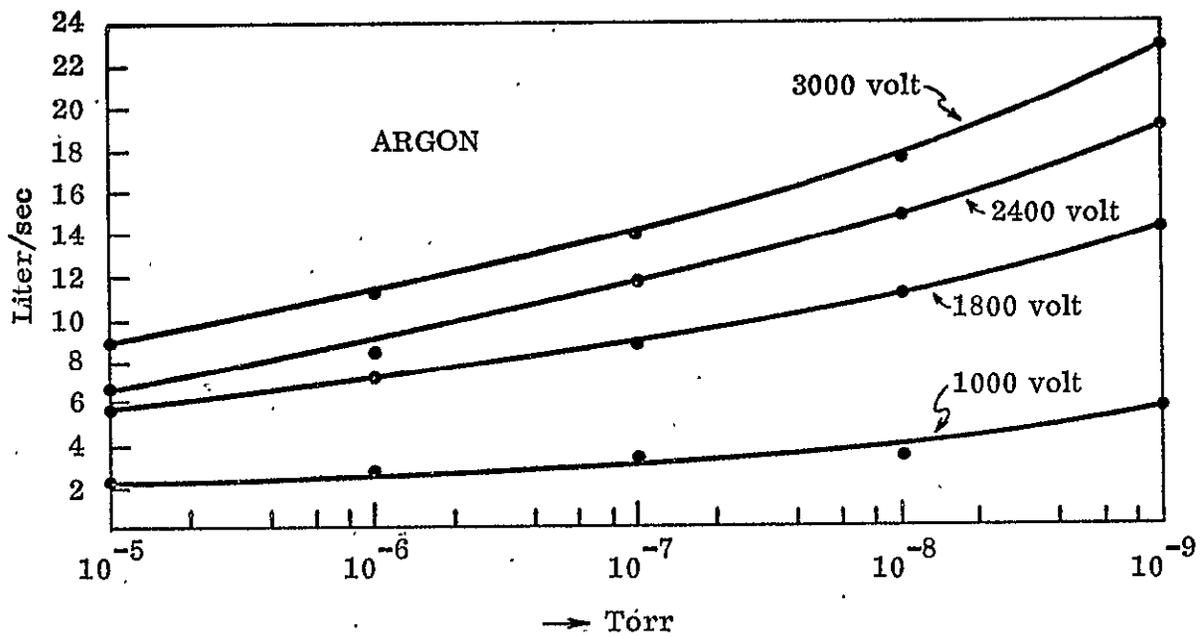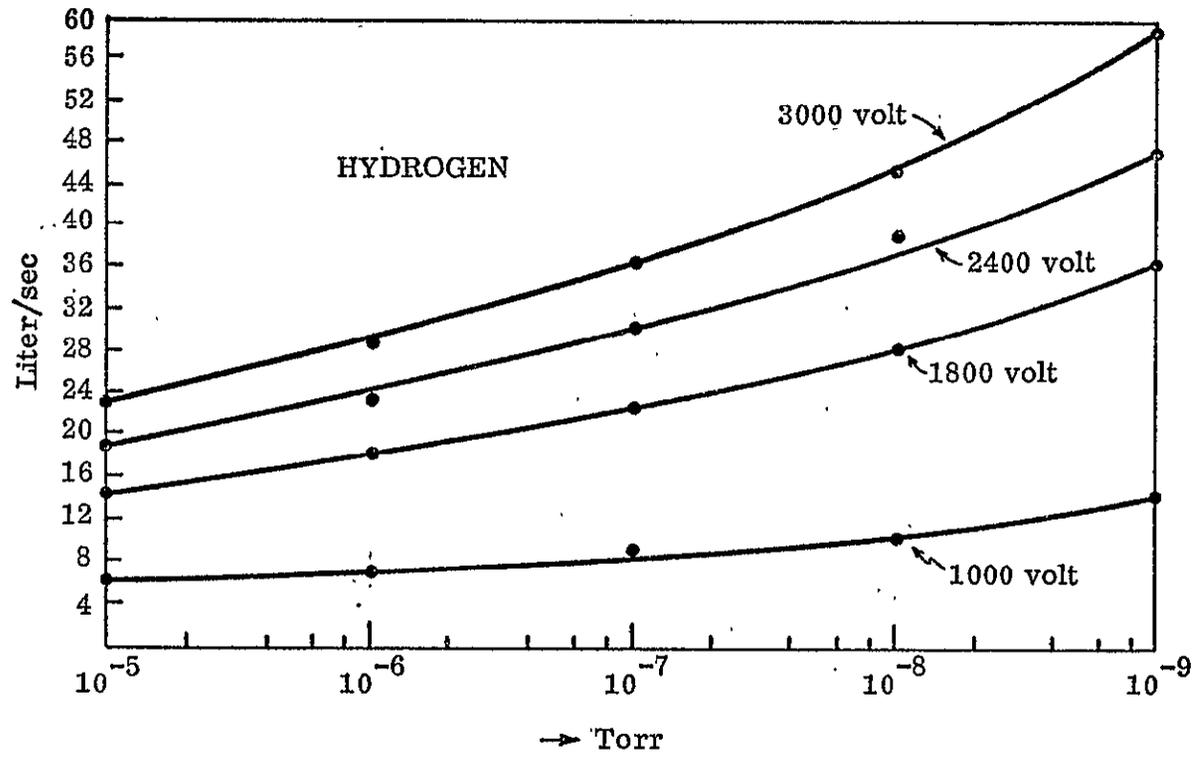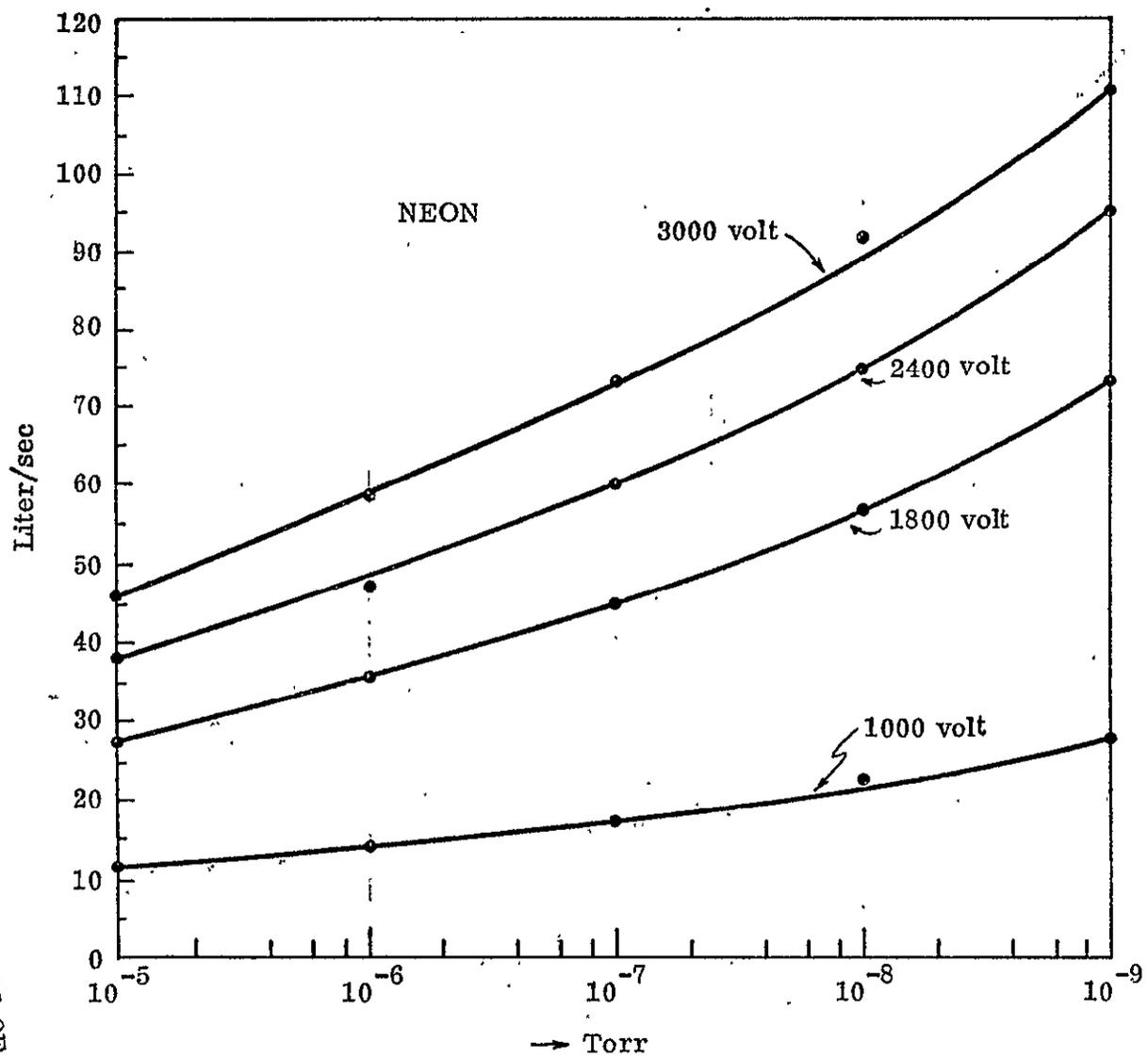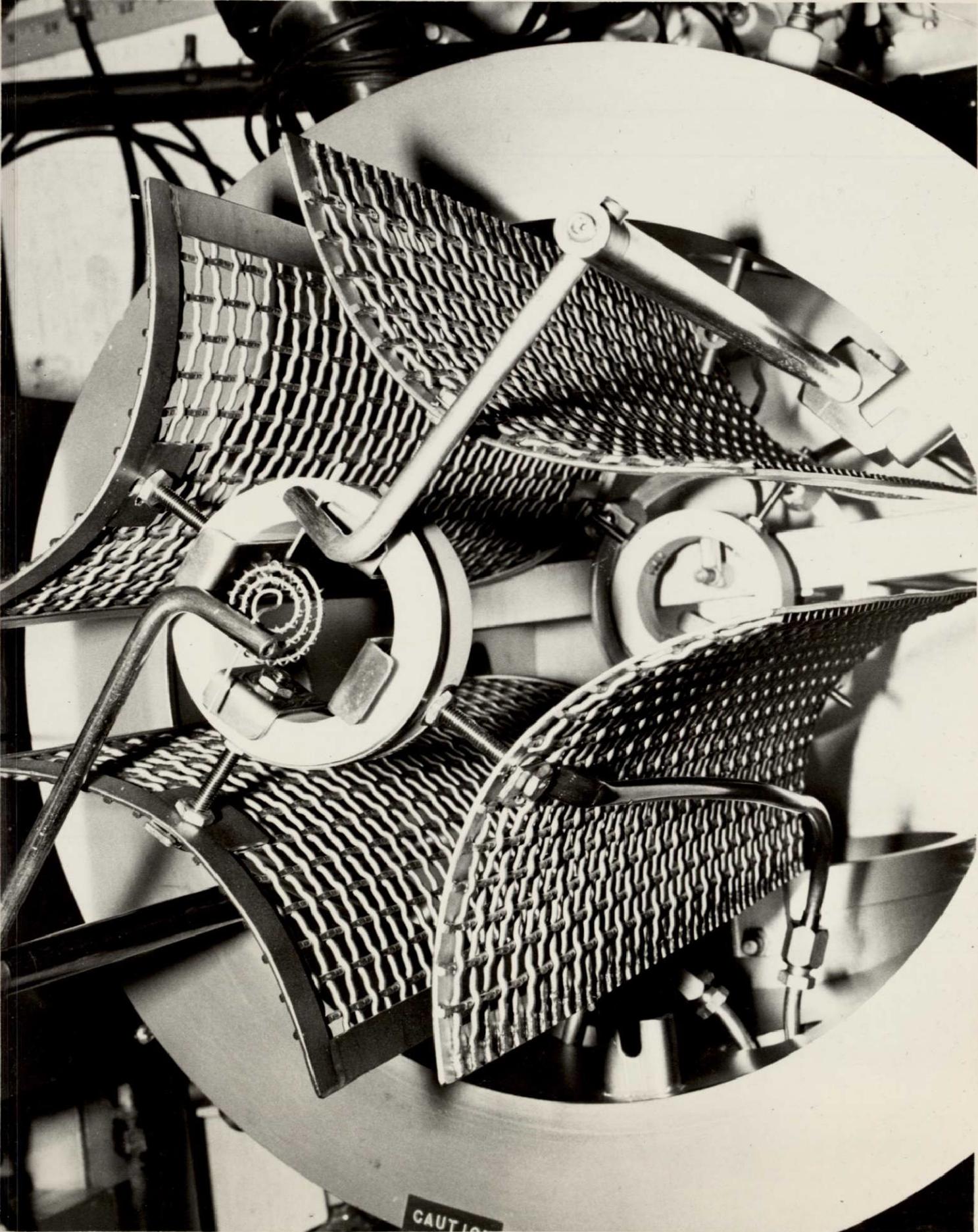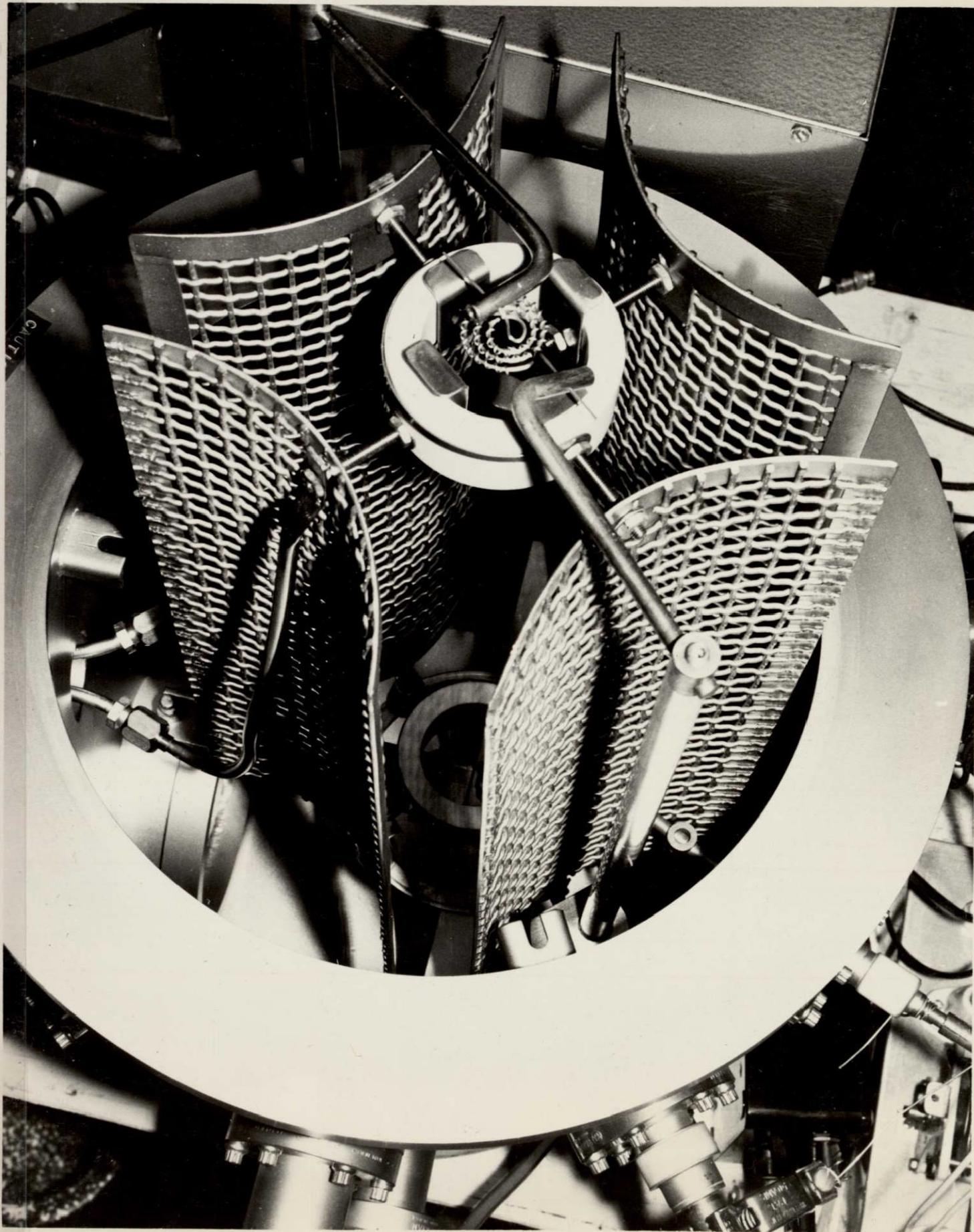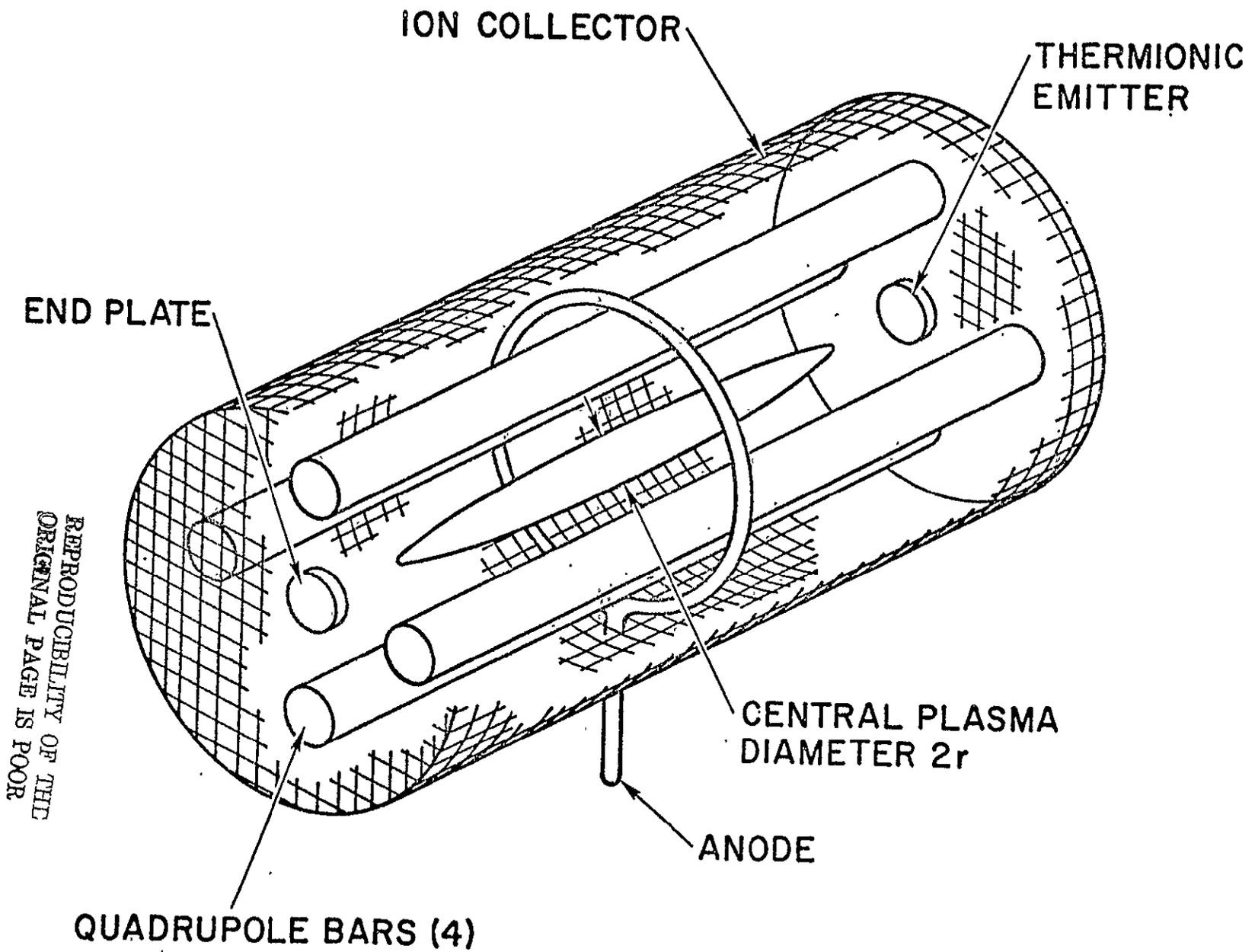
Figure 11

DIAMETER OF PLASMA AS A FUNCTION OF PRESSURE

Figure 12
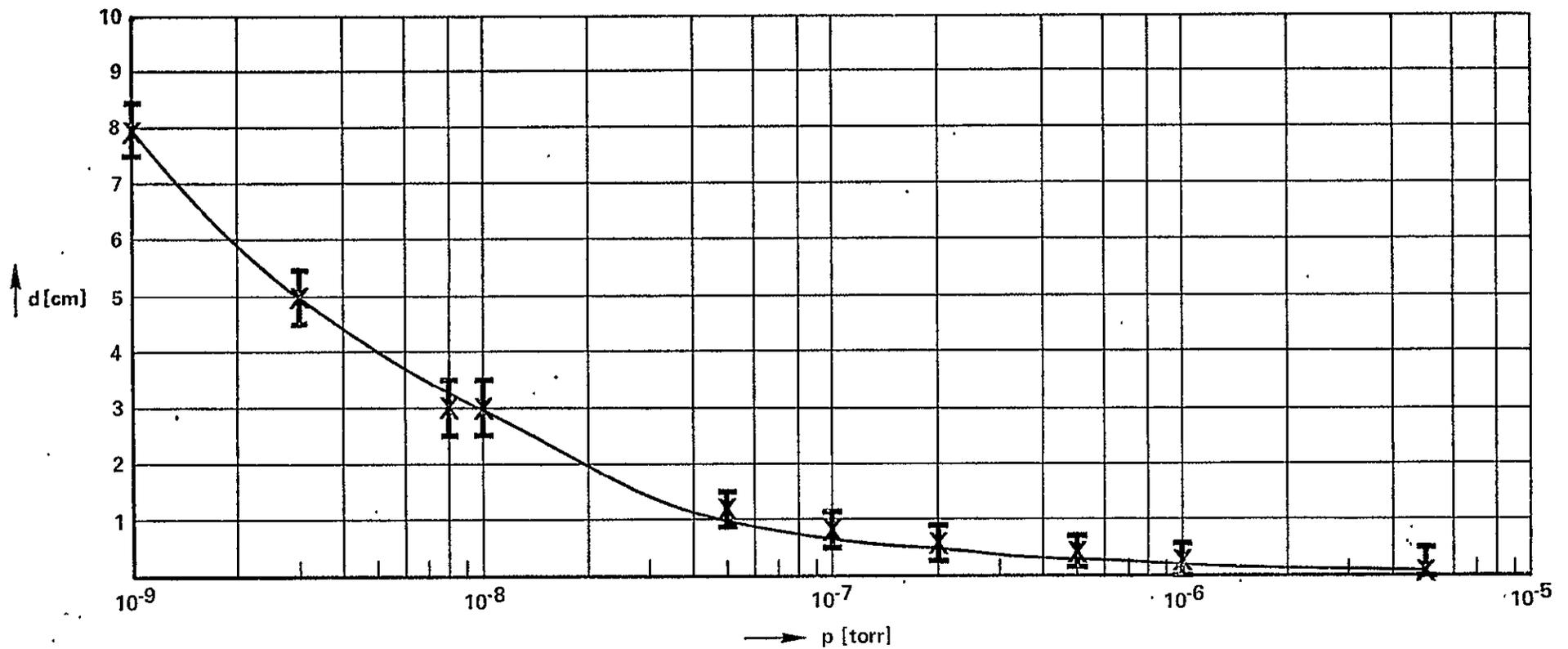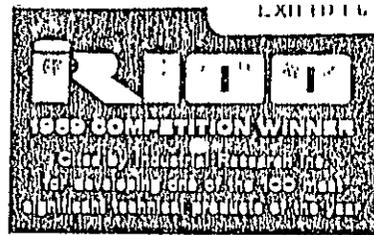
Quadrupole ionization gauge

H. SCHWARZ

Rensselaer Polytechnic Institute, Hartford Graduate Center, East Windsor Hill, Connecticut, U.S.A.

Abstract. The new non-magnetic ionization gauge can be compared with a Penning-type ionization gauge in which the electrons oscillate along the axis of the tube. The main difference between the Penning gauge and the new gauge lies in the fact that the confinement of the electrons is achieved by electrostatic quadrupole lenses instead of a magnetic field. Electrons are emitted from a hot cathode at one end of the tube and accelerated along the tube. They then encounter an inverted field, since at the other end of the tube a flat disk is positioned which has a potential slightly lower than the cathode potential. This causes the electrons to return and continue to oscillate, reaching maximum velocity each time they pass the middle of the tube. The ions produced are collected by a cylindrical screen surrounding the whole electrode structure and/or the flat disk. No fast electrons can hit any solids, so that the x-ray production is kept very low. The tube can be operated in two modes: (1) d.c. potentials or (2) ultra-high frequencies (about 200 MHz) are applied to the quadrupole rods. In the case of d.c. operation, the sensitivity factor was a factor of 10 and in high-frequency operation a factor of more than 2000 higher than that of a regular Bayard–Alpert gauge. The x-ray limit is so low that it plays a lesser role than adsorption and desorption phenomena at the ion collector. Adsorption and desorption processes come into equilibrium in front of the ion collector and create a kind of 'gas cloud'. This had earlier been postulated as the main reason for the lower limit of ionization gauges.

1. Introduction

The new non-magnetic ionization gauge consists basically of quadrupole lens systems excited at high frequency. The principle of focusing with a quadrupole system had already been proposed in 1950 in a patent issued to Christofilos (1950). Independently, Courant et al. (1952) had studied the possibility of using alternating-gradient focusing for particle accelerators, while Paul and Steinwedel (1953) had proposed this same principle for application in mass spectrometry. Many papers have appeared in the meantime on the subject, and a recent survey of them can be found in a book edited by Septier (1967). The quadrupole radio-frequency devices were mostly used for mass filtering, and only recently have Dawson and Whetten (1968) mentioned the possibility of using such a system as an ionization gauge. Already Fischer (1959) had worked out a theory on how to focus electrons with rotationally symmetric quadrupole fields for possible use as an ionization gauge.

The present work differs substantially from the previous efforts in that the quadrupole tube is operated under such conditions that predominantly electrons are being focused by this kind of strong-focusing device. At the other end of the hot cathode the electrons encounter a slightly negative potential and therefore are driven back. The device is somewhat similar to a Penning-type gauge, the electrons being confined in the centre of the tube by strong-focusing quadrupole lenses instead of a magnetic field. The ions produced are collected by a small disk in the centre opposite the cathode; this disk also provides the negative potential for the creation of the inverse field.

2. Principle of operation

Four rods placed symmetrically parallel around the axis of the tube with alternating potential imposed on them produce approximately the same quadrupole field as the ideal configuration of hyperbolic electrodes sketched in figure 1. An a.c. potential $U_0 \cos \omega t$

with a superimposed d.c. potential U_{dc} is applied between a pair of opposite 'rods'. The electric field within the quadrupole is given by

$$E = -\mathrm{grad}\left\{\frac{U_{dc} + U_0 \cos \omega t}{r_0{}^2}\,(y^2 - z^2)\right\} \tag{1}$$

$$m\frac{d^2y}{dt^2}\,j + m\frac{d^2z}{dt^2}\,k = -eE \tag{2}$$

which leads to the following differential equations for y and z

$$\frac{d^2y}{dt^2} - \frac{2e}{mr_0{}^2}\,(U_{dc} + U_0 \cos \omega t)y = 0 \tag{3}$$

$$\frac{d^2z}{dt^2} + \frac{2e}{mr_0{}^2}\,(U_{dc} + U_0 \cos \omega t)z = 0 \tag{4}$$

Both are of the form of Mathieu's equation (see McLachlan (1947))

$$\frac{d^2\zeta}{d\theta^2} + (a - 2q \cos 2\theta)\zeta = 0 \tag{5}$$

the solution of which is given by:

$$\zeta = A \exp(\mu\theta) \sum_{-\infty}^{+\infty} c_\nu \exp(i\nu\theta) + B \exp(-\mu\theta) \sum_{-\infty}^{+\infty} c_\nu \exp(-i\nu\theta) \tag{6}$$

which can be applied for ζ being either y or z. In the first case (equation (3))

$$a = a_y = -\frac{8eU_{dc}}{r_0{}^2 m\omega^2} \tag{7}$$

and in the second case (equation 4)

$$a = a_z = +\frac{8eU_{dc}}{r_0{}^2 m\omega^2} \tag{8}$$

and in both cases

$$q = \frac{4eU_{dc}}{r_0{}^2 m\omega^2} \tag{9}$$

which results from the fact that the time operator d^2/dt^2 has to be replaced by the operator $(4/\omega^2)(d^2/d\theta^2)$, since $\theta = \omega t/2$. The characteristic exponents μ of the solution can be determined from a and q. But in order that y and z may be real, μ has to be purely imaginary of the form $\mu = (b/d)i$, where b and d are integral numbers. The upper limits for a_z and the lower limits for a_y respectively for which these conditions exist are represented by the two curves in figure 2; a_z and a_y are already given in units of U_{dc} as a function of the peak voltage U_0 for electrons and at a high frequency of $\nu = 200$ MHz as applied to
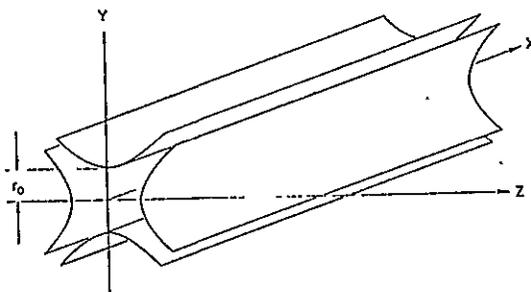

Figure 1. Ideal electrode configuration for quadrupole field.

the rods. So that only electrons remain on a stable trajectory, one has to stay close to the two points of the two curves which yield $a_y = -a_z$. This is the case approximately at $U_0 = 160$ v, which then fixes the value for $U_{dc} = 27$ v. For values of $U_0 > 160$ v, one still have stable trajectories for electrons, but other charged particles with higher masses M may also become stable. The d.c. potential U_{dc} then to be applied can be determined from the intersection of the line as given by $U_{dc} = -\gamma U_{01}$ with the lower curve of figure 2. γ is smaller than $0\cdot166$ and U_{01} varies between 0 and U_0. From the corresponding value for U_{01} one can find the range of masses up to which stable conditions exist. All charged particles with atomic weights smaller than

$$A = 5\cdot45 \times 10^{-4}\, U_0/U_{01} \tag{10}$$

then fulfil these conditions for the constructed device with $r_0 = 1$ cm and $\nu = 200$ MHz.
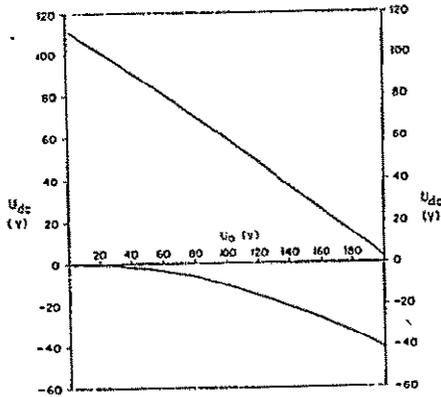

Figure 2. Stability limits for quadrupole field. Units in volts for electrons, $r_0 = 1$ cm and $\nu = 200$ MHz.

For ions with $A = 1$ (hydrogen), a ratio of $\gamma U_0/U_{dc} \simeq 1840$ would be necessary, which shows that with $\gamma < 0\cdot166$ practically only electrons will oscillate under stable conditions. Owing to the long electron path, the number of ions produced will be much higher than in a normal ionization gauge.

3. Gauge design and electrical circuit

The schematics of the quadrupole ionization gauge with its electrical connections are depicted in figure 3. The four rods R provide the alternating high-frequency field. Electrons are emitted from the hot cathode C, which consists of a pure tungsten wire in hairpin shape. At the anode ring (AR) the potential U_{dc} is applied and serves mainly to detect the electron emission i^- in an amperemeter A before the high frequency is set in operation. The collector disk Co has a potential V_0 negative against the cathode. Ions
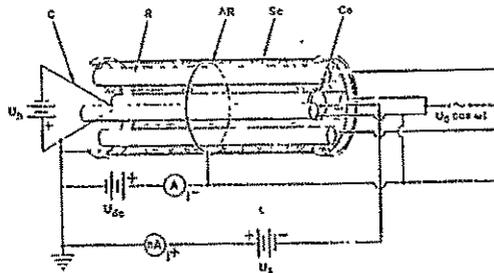

Figure 3. Schematics of quadrupole ionization·gauge and electrical circuit.

being collected at Co are measured as a current i^1 with an electrometer-type nanoammeter (nA).

In order to avoid transmission losses at the relatively high frequency, the two pairs of the quadrupole rods were used as transmission lines for the high frequency. This is not shown in figure 3. To obtain the peak-to-peak voltage between the two pairs of rods, an appropriate impedance (not shown in figure 3) was inserted at the other end of the rods. The whole electrode structure is enclosed by a cylindrically shaped screen which is at ground potential, as is the positive side of the cathode C heated by a low-voltage d.c. power supply U_h. The peak voltage U_0 is also measured by an r.f. voltmeter not shown in figure 3.

4. Calibration of gauge

It was possible to find the conditions under which the ion current i^1 was proportional to the pressure p and the electron current i^-, as this latter was determined before the r.f. generator had been set in operation.

The pressure p was determined with a Redhead gauge. The vacuum was produced with an Ultek-ion pumping system which had been rough-pumped with a cryopump. Stainless steel was used throughout for the construction of the vacuum system. Copper gaskets for the flanges and valves were used that could be baked out up to 450°c. After proper ultra-high-vacuum treatment, an ultimate vacuum of 10^{-13} torr could be obtained. Calibration was performed with dry air and argon.
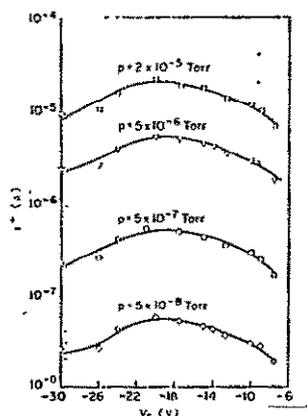

Figure 4. Ion current i^+ as a function of collector potential V_s at different pressures p of dry air for $U_0=160$ v, $U_{dc}=27$ v, $\nu=200$ MHz.

Figure 4 shows a family of curves giving a relationship as measured between the ion current i^+ and the collector potential V_s for different pressures of dry air as parameters starting from 2×10^{-5} torr down to 5×10^{-8} torr. For the optimum collector potential of about $V_s=-19\cdot5$ v, the gauge constant C as defined by

$$Cp=i^+/i^- \tag{11}$$

revealed a value of $C\simeq10^4$ torr^{-1}. Under d.c. conditions, which means the rods were only at the potential U_{dc}, this constant did not exceed a value of $C\simeq50$ torr^{-1}. This is a factor of 10 higher than the VEECO-type Bayard–Alpert gauge.

5. Lower limit

The lower limit for the r.f. operation has not yet been determined. Down to 10^{-13} torr a linear relationship between pressure p and ion current i^+ could still be observed. However, quite a pumping action could be found, and there are indications that the lower

limit is not determined by x rays eventually produced by the slow electrons, but rather by absorption and desorption processes at the collector electrode. These processes enter into equilibrium in front of the ion collector and create a kind of 'gas cloud', as earlier ●tulated by Schwarz (1951) (see also Haefer 1955) and apparently later observed by ●lhead (1966). Such a gas cloud, being in a steady state, may be the main effect that determines the lower limit long before the x-ray limit shows up.

References

CHRISTOFILOS, N. C., 1950, U.S. Patent No. 2 736 799 (issued Feb. 28, 1956).

COURANT, E. D., LIVINGSTON, M. S., and SNYDER, H. S., 1952, *Phys. Rev.*, **88**, 1190–6.

DAWSON, P. H., and WHETTEN, N. R., 1968, *J. Vacuum Sci. Technol.*, **5**, 1–18.

FISCHER, E., 1959, *Z. Phys.*, **156**, 1–26.

HAEFER, R., 1955, *Acta Phys. Austr.*, **9**, 200–15.

McLACHLAN, N. W., 1947, *Theory and Application of Mathieu Functions* (London and New York: Clarendon Press).

PAUL, W , and STEINWEDEL, H., 1953, *Z. Naturforsch.* A, **8**, 448–50.

REDHEAD, P. A., 1966, *Abs. 13th A.V.S. Nat. Vacuum Symp.* (Pittsburgh, Pa.: Herbick and Held), 67–8.

SCHWARZ, H., 1951, *Arch. Techn. Messen (ATM)* V–1341–2.

SEPTIER, A., 1967, *Focusing of Charged Particles*, Vol. II (New York: Academic Press).
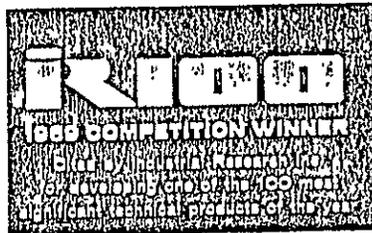
Inverse Pressure Dependence of the Quadrupole Ionization Gauge

Helmut Schwarz and H. A. Toutellotte

Inverse Pressure Dependence of the
Quadrupole Ionization Gauge*

Helmut Schwarz and H. A. Tourtellotte

*Rensselaer Polytechnic Institute—Hartford Graduate Center,
East Windsor Hill, Connecticut 06028*
(Received 12 August 1968)

A nonmagnetic ionization gauge has been developed in which electrons are oscillating back and forth along the axis of the tube as in a Penning type ion gauge. The electrons are emitted from a hot hairpin filament at one side of a cylindrical tube and are accelerated by a dc potential of 27 V towards the other end. At the other end there is a disk-shaped electrode which has the same potential as the cathode. This causes the electrons to travel back and forth between the ends until they suffer a collision. A quadruple system serves to keep the electrons from reaching the electrodes and the wall. The system is excited by a rf oscillator of 200 MHz and 165 V peak voltage which is tuned in such a way that only electrons will not deviate from stable trajectories along the center of the tube. A closed screen surrounds the whole electrode structure. It is at a slightly negative potential and serves as the ion collector. Within the pressure range $p = 10^{-6}$ to 10^{-10} Torr the ion current i follows the relationship $pi^n = c$. n was found to be 1.31 ± 0.02 for electron emissions of 10, 50, 100, and 500 μA. The constant c was $c = 2.88 \times 10^{-17}$ for 10 μA, 2.63×10^{-16} for 50 μA, and in the case of 100 μA it was 5.37×10^{-15}.

Introduction

There were three main considerations given to the conception of the quadrupole ionization gauge[1]: (1) It should have a low x-ray limit, which would imply that very few electrons of appreciable energy should impinge on solid surfaces. (2) A magnetic field should be eliminated. (3) The ionizing electrons should travel as long as possible within the gauge volume. These three points were achieved by the construction of a double quadrupole system. The new gauge resembles a Penning type ion gauge device. The main difference is that instead of using a magnetic field for keeping the electrons in the center of the tube, one uses quadrupole optics. Other attempts to use the quadrupole arrangement as an ion gauge have been reported by G. Rettinghaus[2] as well as P. H. Dawson and N. R. Whetten.[3] Their devices, however, were tuned for ions in a three-dimensional, rotationally symmetric, quadrupole field. In order to extract the ions for pressure measurements, drawout pulses as high as 400 V during 2-5 μsec intervals had to be applied. However, no steady measurement could be performed.

The quadrupole system is actuated by a radio frequency oscillator and tuned so that only electrons

are moving on stable trajectories within the center of the tube. A dc potential is superimposed on the radio frequency and also applied to a ring-shaped electrode positioned halfway. At the other end of the tube, the electrons will encounter an inverse field due to a disk electrode which is at the same potential as the cathode. The electrons will remain in the tube until they hit gas atoms or molecules. They will then scatter with a probability of ionizing. Some of the ions are collected at a screen surrounding the entire electrode structure. It was completely unexpected that the "ion current" arriving at the screen would increase with decreasing presssure within the range of 10^{-6} to 10^{-10} Torr. At this time, we cannot offer a satisfactory theory to explain this abnormality. However, a possible explanation may be the coupling of the high electron space charge to the collector grid, which might change with pressure. The increase of the "ion current" obviously cannot indefinitely continue with decreasing pressure. There should be a turning point, probably below 10^{-10} Torr. Indications are that this turning point is relatively sharp at 10^{-11} Torr for an initial electron emission of 100 μA.

1. Theory of rf Actuated
Quadrupole Lens for Electrons

Most quadrupole arrangements are used for mass spectrometry and were first introduced for this purpose as an electrical mass filter by W. Paul and H. Steinwedel.[4] The theory of quadrupole systems has

---

[1] H. Schwarz, "Quadrupole Ionization Gauge," Proc. 4th Internat. Vac. Congress, Manchester, England, 1968 (to be published). Inst. Phys. and The Physical Society, London.
[2] G. Rettinghaus, Z. Angew. Phys. 22, 321 (1967).
[3] P. H. Dawson and N. R. Whetten, J. Vac. Sci Technol. 5, 1, 11 (1968).
[4] W. Paul and H. Steinwedel, Z. Naturforsch 8a, 448 (1953).
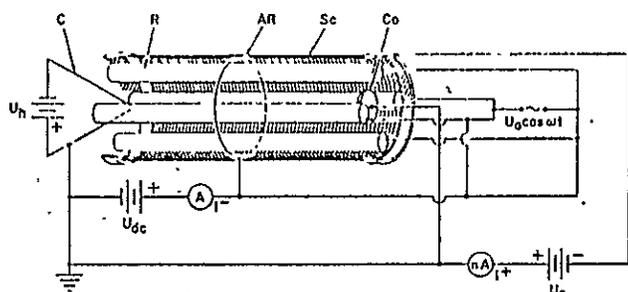
Figure 1. Schematics of quadrupole ionization gauge and electrical circuit.

been treated by several authors, for example by W. Paul and M. Raether.[5] The specific equations of electron movement in a quadrupole tube as illustrated in Fig. 1 have been outlined in a previous paper.[1] They lead to Mathieu's equations. The x-coordinate is the axis of the tube, see Fig. 1. y and z coordinates are the other Cartesian coordinates passing through the center of opposite pairs of rods. r_0 is the inner radius of the quadrupole arrangement, see Fig. 1. The solutions of Mathieu's equations[6] are only real if a_y is not larger than

$$a_y = -BA^2 U_0^2 \left(\frac{1}{2} - \frac{7A^2 U_0^2}{128} \right), \qquad (1)$$

and a_z is not smaller than

$$a_z = B \left(1 - A U_0 - A^2 U_0^2 + \frac{A^2 U_0^2}{64} - \frac{A^4 U_0^4}{1536} \right), \qquad (2)$$

where $A = 1.77(10 r_0 \nu)^{-2}$; $B = 28 r_0^2 \nu^2$; r_0 in meters, ν in MHz; U_0 a_y and a_z in volts.

In our gauge we used a frequency of $\nu = 200$ MHz which determines the ratio of the peak voltage U_0 and the superimposed dc voltage U_{dc}. For electron focusing when $a_y = -a_z$ the ratio U_0/U_{dc} equals 6.05. This means that for a peak voltage of $U_0 = 165$ V, the dc potential should be $U_{dc} = 27$ V. Our device has always been tuned for maximum collector (Sc) current which coincided with the theoretical relationship for best electron focusing. The electrodynamics will only be valid if electrons are free to move. As soon as the electrons hit a gas atom or molecule, they will deviate from the desired movement. Under ideal conditions the unperturbed electrons will move indefinitely back and forth along the trajectories. The number of unperturbed electrons will increase as the pressure decreases. At pressures of 10^{-13} Torr an electron will have a mean free path of 10^{10} cm. An electron of such a long mean free path will travel back and forth in the tube as long as "8 min" until it suffers a collision, which could lead to ionization. Assuming a

[5] W. Paul and M. Raether, Z. Physik 140, 262 (1955).
[6] N. W. McLachlan, *Theory and Application of Mathieu Functions* (Oxford Press, London, 1947).

10% probability for such an event at a pressure of 10^{-13} Torr, an "ion current" of the order of microamperes can be expected. We have reached such high ion currents in our experiments.

II. Experimental Set-Up and Results

A. Description of Quadrupole Ionization Gauge

Figure 1 shows a schematic drawing of the gauge. The screen Sc collects the ions which were measured in a Keithley Electrometer model #610B. The optimum negative potential was $U_s = -77$ V against the cathode. The disk Co was connected with the cathode C. The cathode was a hairpin filament heated by a dc power supply. The ring AR was connected with the four rods R and had a potential of $U_{dc} = +27$ V. A simple milliamperemeter A was inserted to measure the initial electron emission i^-. The radio frequency was fed into the rods by using the rods themselves as transmission lines. The peak voltage was obtained by inserting an impedance between two pairs of opposite rods. All electrodes except for the cathode were constructed from nonmagnetic stainless steel, and were mounted on fixtures of aluminum oxide. The whole structure was mounted on a stainless steel flange with ceramic feedthroughs, and attached to a stainless steel tube. The flange was tightened to the tube with a copper sealing ring. The total length of the electrode structure was 10 cm, and the internal radius as defined above was $r_0 = 1$ cm.

B. Calibration System

For calibration a dry ultrahigh vacuum system was used (Ultek system 25 liter/sec pumping speed). It consisted of an Ultek Boostivac Ion Pump backed up by a sorption pump. The entire system was constructed with stainless steel flanges which were sealed with copper rings and Granville–Phillips type bakeable valves. It was, therefore, possible to bake the system at 400°C.

C. Calibration Procedure and Results

The quadrupole ionization gauge was compared with a Redhead gauge. It was calibrated with dry air and argon at room temperature. Two different procedures were used for calibration: (a) in a static closed system, and (b) in a dynamic system where an equilibrium between pumping speed and gas inlet was maintained to establish a certain pressure.

1. Procedure a: Before calibration, the main valve was closed to disconnect the system from the ion pump. A needle valve was used to let the gases into the system up to a certain pressure and after stabilizing, the pressure was measured and the optimum ion current as collected by the screen Sc, see Fig. 1, was noted.
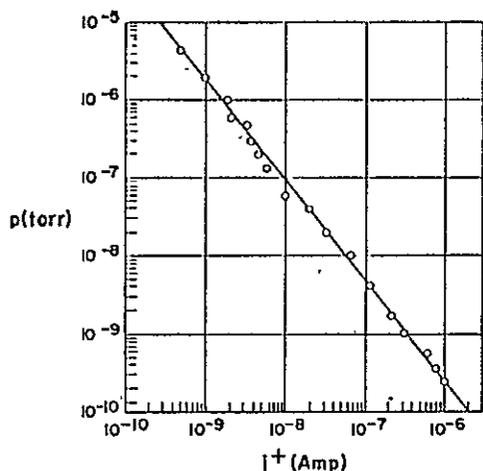
Figure 2. Calibration curve with screen as ion collector at low rf power (approximately 20 W).

Figure 3. Calibration curve with screen as ion current collector for different electron emissions at high rf power (approximately 40 W).

2. *Procedure* b: Another way the system was calibrated was by leaving the main valve open and having the needle valve throttled until a certain pressure was stabilized due to the continuous pumping of the ion pump. The spread of the measured points on Figs. 2 and 3 is due to the slight pumping action.

Procedures (a) and (b) essentially did not show any noticeable difference on the calibration curves.

Calibration curves were measured at different rf power imputs and different electron emission currents. By adjusting the power supply for heating the filament, the emission current was set with only the dc potentials on. After feeding in the rf frequency with the correct peak potential, the emission current as measured at the milliamperemeter A, see Fig. 1, dropped down to 1% to 10% of its initial value. This means that due to electron focusing and oscillations a negative space charge built up and prevented further electron emission of the cathode. A high ac current existed within the center of the tube. The fact that the emission current dropped to such a low value means also that very few electrons of high energy really hit solid parts in the tube. Figure 2 corresponds to a calibration at an initial electron emission of 100

i^- (μA)	n	c
10	1 31	2.88 × 10⁻¹⁷
50	1.33	2 63 × 10⁻¹⁶
100	1.29	5 37 × 10⁻¹⁶

μA and an rf power transmitted into the quadrupole gauge of about 20 W. The exponent n of Eq. (1) was found to be equal to 1.30 and the constant $c = 3.83 \times 10^{-18}$. Figure 3 depicts three calibration curves at three different initial electron emission currents of 10, 50, and 100 μA, and higher rf power of about 40 W. The calibration constants n and c for the three initial electron emission currents are listed on Table I. As one can see from Figs. 2 and 3, the inverse pressure dependence still held in the pressure range from 10^{-5} to 10^{-10} Torr and there is not any indication that the ion current will decrease with decreasing pressure.

The inverse mode of operation is very desirable for measuring very low pressures since currents in the range of microamperes are being measured. This does not raise any insulation problems with our quadrupole ionization gauge whereas most other vacuum gauges have this problem in the very low pressure range.

III. Pumping Action

It was noticed that the quadrupole ionization gauge pumps as most other ionization gauges. This was observed even when the gauge was operating under dc conditions. In the case of dc operation, a pumping speed of 0.1 liter/sec was observed and in the rf operation 0.4 liter/sec.

Acknowledgments

U. S. DEPARTMENT OF COMMERCE
UNITED STATES PATENT OFFICE

September 21, 1972
(Date)

THIS IS TO CERTIFY that the annexed is a true copy from the records of this office

of printed Specification and Drawings of U. S. Patent 3,665,245.
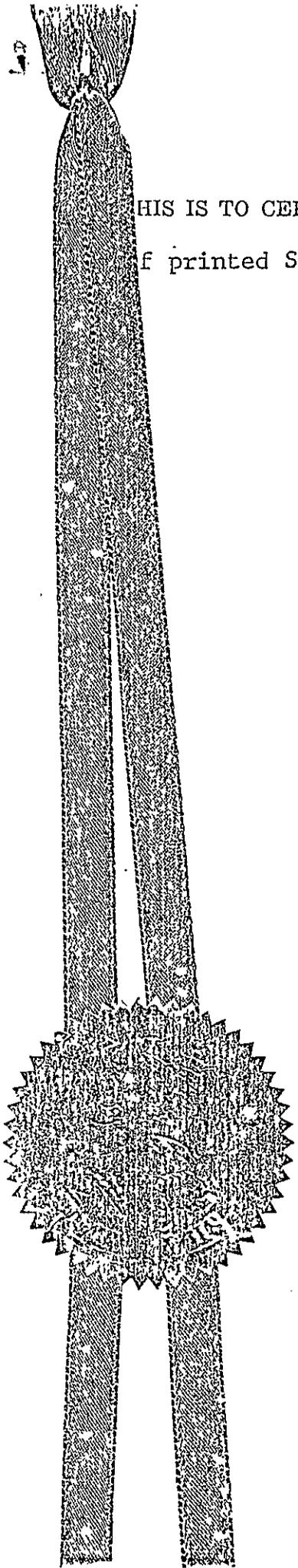
By authority of the
COMMISSIONER OF PATENTS

Certifying Officer.

[57] **ABSTRACT**

A non-magnetic ionization gauge or ion pump comprising a tube containing spaced cathodes at the same potential, with an intermediately positioned ring anode for setting up an oscillating stream of electrons that is focused or constrained within an axial path by an electric quadrupole lens arrangement which may be excited by the RF force. The quadrupole lenses create a field which is tuned firstly to lengthen and stabilize the path of the electrons thus causing greater ionization of the gas atoms in the tube, and also to expel the ions produced thereby, which ions are then collected by a cylindrical collector screen at a slightly negative potential surrounding the whole electrode structure. The collector current produced with this arrangement has been found to be approximately inversely proportional to the pressure within the range from 10^{-5} to 10^{-10} torr, so that collector currents of the order of microamperes can be obtained at very low pressure levels

10 Claims, 9 Drawing Figures
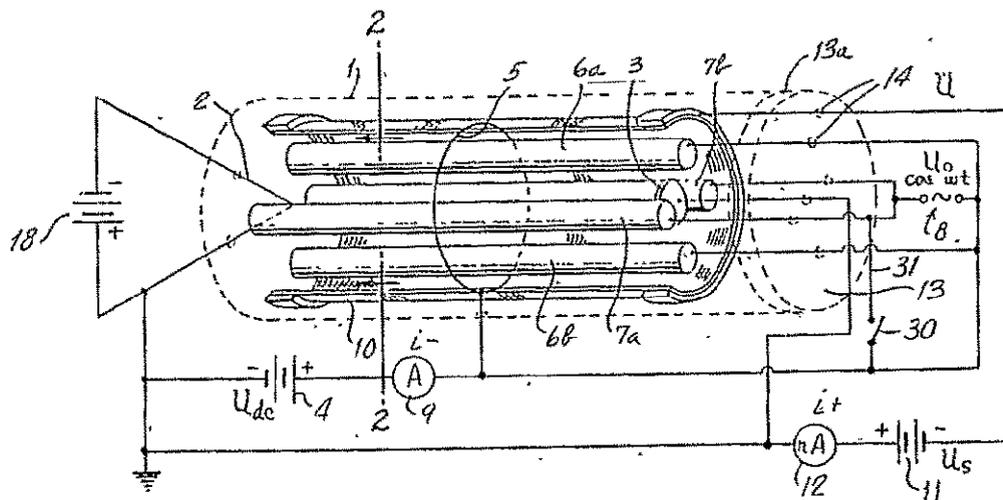
Fig. 1.

Fig. 1a.

Fig. 2.

QUADRUPLE
IONIZATION
GAUGE

REDHEAD
IONIZATION
GAUGE

Fig. 3.

CALIBRATION
PRESSURE
CHAMBER

NEEDLE
VALVE

ATMOSPHERE

MAIN
VALVE

Fig. 4.

ION
PUMP

FORE
PUMP

INVENTOR
HELMUT J. SCHWARZ

BY

ATTORNEY

Fig. 5.

p(torr)

$i = 100\ \mu A$
$\nu = 200\ MHz$
POWER = 20 WATTS

COLLECTOR CURRENT i^+ (AMP)

Fig. 8.

Fig. 6.

p(torr)

○ $i = 10\mu a$
□ $i = 50\mu a$
△ $i = 100\mu a$
$\nu = 200\ MHz$
POWER = 40 WATTS

COLLECTOR CURRENT i^+ (AMP)

Fig. 7.

INVENTOR.
HELMUT J. SCHWARZ
BY

ATTORNEY

1
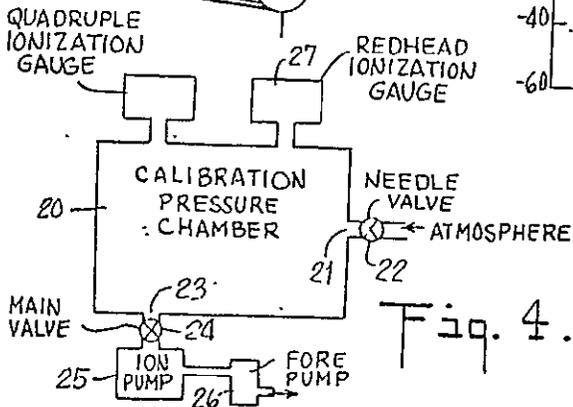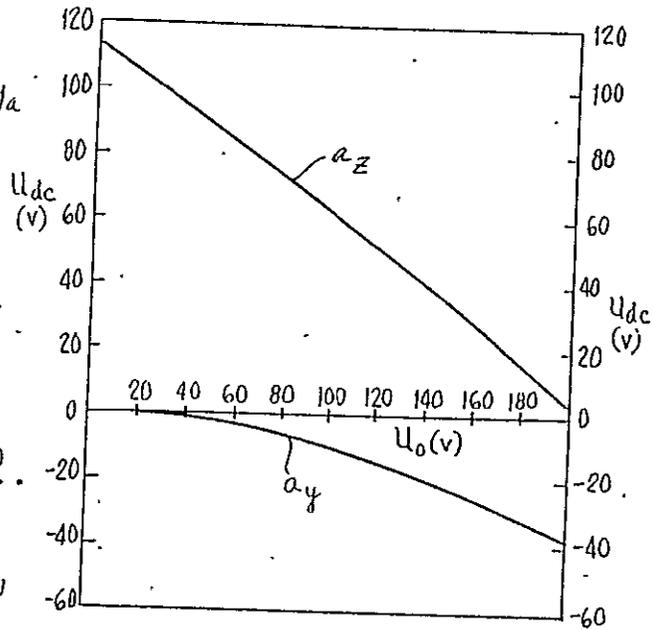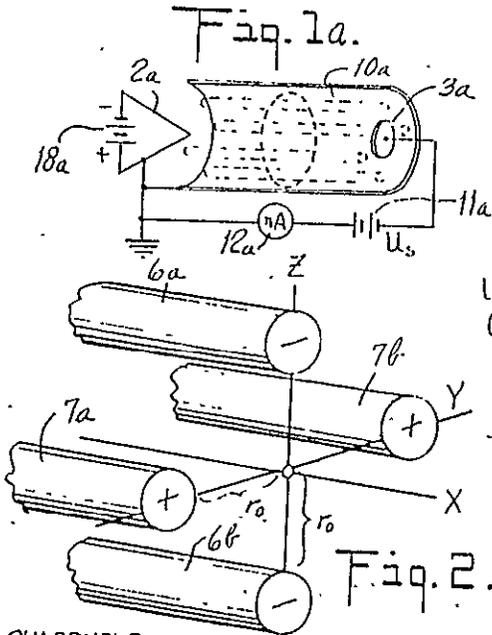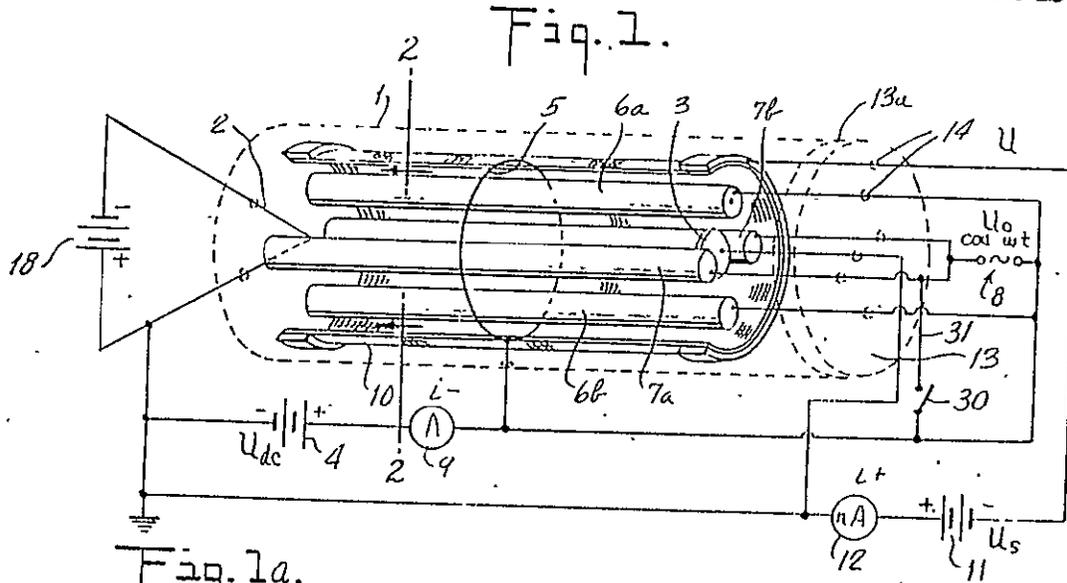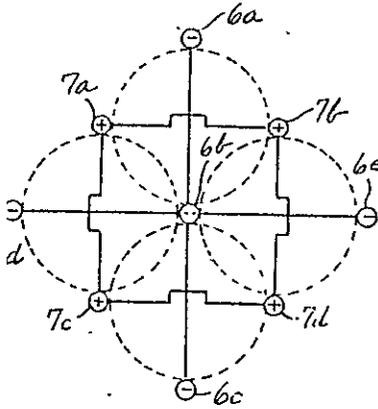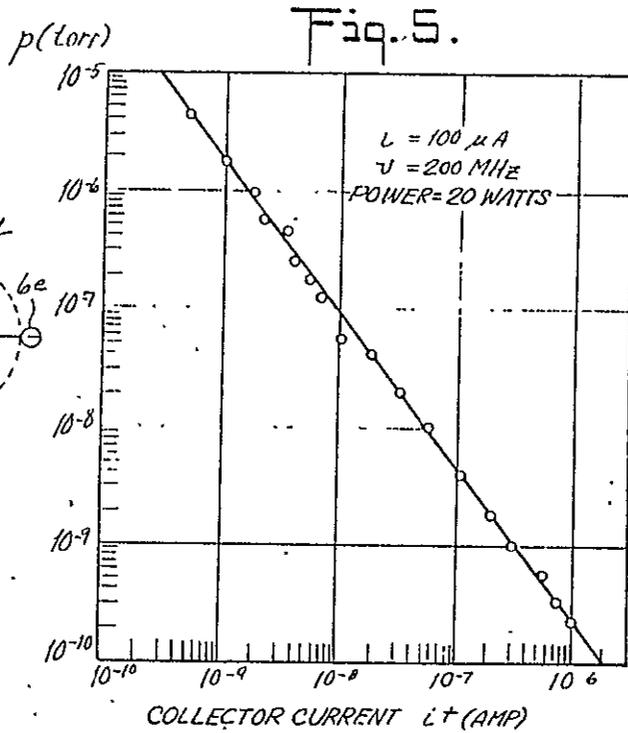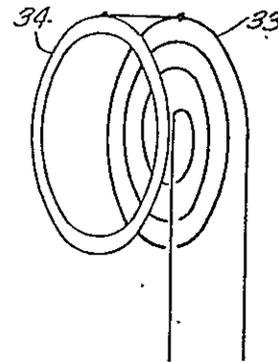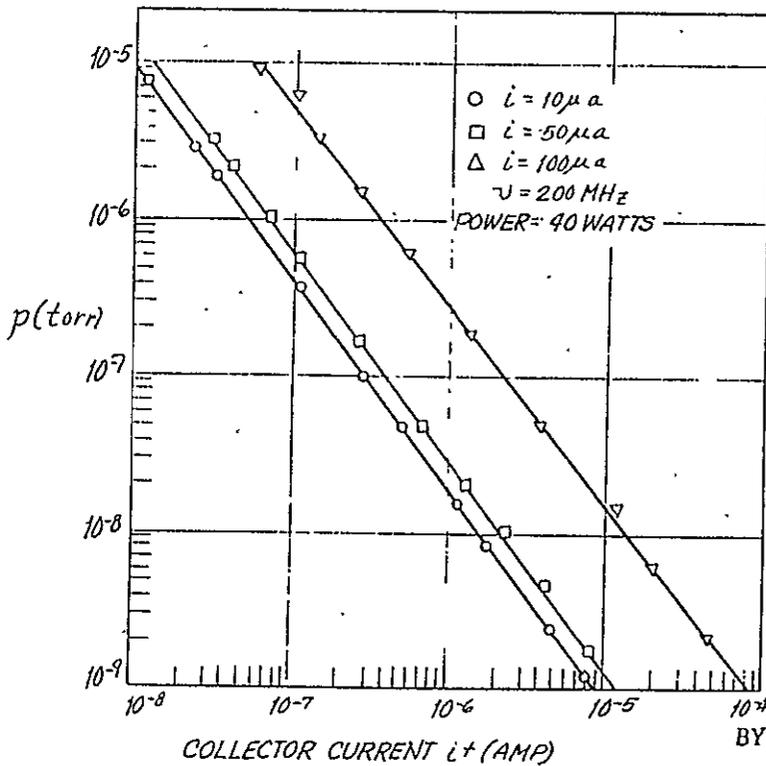
QUADRUPOLE IONIZATION GAUGE

BACKGROUND OF THE INVENTION

The present invention relates to vacuum gauges of the ionization type and particularly to a non-magnetic ionization vacuum gauge or ion pump, using electric quadrupole focusing of the ionizing electron stream.

The creation and measuring of vacua by electron impact ionization of gas atoms present in a given enclosure has been known for some time. At present several ionization gauges of this type are available for measuring low pressures down to less than 10^{-11} torr, most of which utilize magnetic fields to increase the length of the electron path by spiralling thus raising the probability of electron-atom collision to improve the degree of ionization. However, all these gauges require a magnetic field in the order of 500 to 2,000 gauss, and the presence of a magnetic field in many measuring applications is undesirable, especially when working with the evaporation of magnetic materials to be laid down in thin films or in electron diffraction studies, particularly with low energies. In addition, the permanent magnets which are frequently used to produce the field are undesirable because of their weight.

Non-magnetic gauges of the orbitron type have been developed wherein the electrons are emitted somewhat off axis at the end of a cylindrical tube with an axial rod which is at positive potential. The immediate vicinity of the electron emitter is shielded against the rod so that the electrons do not go directly to the rod, but spiral around it. However, in these devices, the electron path cannot be increased as much as in a well-designed magnetic gauge and other features make them difficult to control. Many electrons are also lost by hitting the rod.

The present invention presents a gauge for measuring very low total gas pressures, particularly within the range of 10^{-5} to 10^{-10} torr, without the use of a magnetic field and which gauge is more sensitive at the low pressure range. In contrast to all other known ionization gauges, the collector current produced is almost inversely proportional to the pressure in this operational range.

SUMMARY OF THE INVENTION

The present invention embodies an ionization gauge or ion pump comprising an electrode structure having spaced cathodes at approximately the same potential, with an intermediately arranged ring anode for establishing an axially oscillating electron stream. The stream is acted upon by a field produced by a set of quadrupole electrodes, which may be electrostatic or also excited by a high frequency voltage, causing only electrons to stay within stable trajectories along the axis of the tube. The oscillating electrons, as a result of the strong quadrupole focusing, have a comparatively long path of travel, so that the number of ions produced by collisions will be much higher than in prior ionization gauges and the resulting ions will be expelled by the quadrupole field. The ions may be collected by a cylindrical collector screen, at a slightly negative potential, arranged to surround the whole electrode structure.

It has been found that with the present gauge using the cylindrical screen, the screen or collector current as a function of pressure follows the simple relationship $p \times i^n = $ const at a given electron emission, where n is a constant exponent of approximately 1 3 with p as the pressure in torr and i the collector current in amperes. Collector currents of the order of microamperes can be obtained at a pressure of 10^{-10} torr, so that the insulation problems involved with prior low pressure ionization gauges are obviated.

While the embodiment as above-described is preferred the gauge may be operated on other modes which are also of improved sensitivity over the prior art devices.

BRIEF DESCRIPTION OF THE DRAWINGS

FIG. 1 is a diagrammatic view of an ionization gauge constructed in accordance with the present invention;

2

FIG. 1a is a diagrammatic view of a modification of the gauge shown in FIG. 1;

FIG. 2 is a view of the quadrupole electrodes in section taken along the lines 2—2 in FIG. 1 and indicating the coordinate axes of the quadrupole field;

FIG. 3 is a plot of the stability limits of the quadrupole field of the ionization gauge of FIG. 1 for an electrode radius $r = 1$ cm and a frequency of $\nu = 200$MHz for the field,

FIG. 4 is a diagrammatic view of a vacuum system used in calibrating the gauge of the present invention,

FIG 5 is a calibration curve of the ionization gauge of FIG. 1, using a quadrupole RF field of approximately 20 watt power;

FIG 6 is a calibration curve of the ionization gauge of FIG. 1, using a quadrupole RF field of approximately 40 watt power,

FIG. 7 is a diagrammatic view of a modification of the reflector cathode of the gauge of FIG. 1 to permit its use as an ion pump,

FIG 8 is a diagrammatic view of a quadrupole electrode arrangement which may be used to construct a multicell ion pump.

DETAILED DESCRIPTION OF THE INVENTION

An ionization gauge constructed in accordance with the present invention is shown diagrammatically in FIG 1. The gauge comprises a cylindrical casing or tube 1 containing a hot cathode 2 and a reflector cathode 3, which are maintained at the same potential such as by connecting them to the negative terminal of a battery 4, or other power supply. The hot cathode 2, which may be in the form of a hot hairpin, heated by a DC power supply 18, emits electrons into the region between itself and the reflector cathode 3 A ring-type anode 5 is disposed in this region, intermediately between the hot cathode 2 and the reflector cathode 3, and is connected to the positive terminal of the battery 4, or other power supply, so as to accelerate the emitted electrons generally along the axis of the electrode arrangement. The accelerated electrons upon passing through the ring anode 5 will be decelerated and repelled by the negative potential on the reflector cathode 3 and will thus be caused to travel back and forth between the hot cathode 2 and reflector cathode 3 until they suffer a collision with the atoms of any gas present along the path within the casing 1

The electrons are maintained within their path of oscillation by a quadrupole lens system comprising a set of quadrupole electrodes, in the form of rods 6a, 6b and 7a, 7b, positioned symmetrically about the path of electron travel. A DC potential equal to U_{dc} of the ring anode 5, is applied to the rods such as by also connecting them to the positive terminal of the battery 4, or other power supply. In addition, an AC potential $U_o \cos \omega t$ of a comparatively high frequency, such as RF, may be applied between the pairs of opposite rods by connection with an AC power source or generator 8. In order to avoid transmission losses at the relatively high frequency, the two pairs of rods may be used as transmission lines. A simple amperemeter 9 may be inserted in the line on the side of the positive terminal of the battery 4 to measure the initial electron emission (i^-) prior to turning on the electric field

When the quadrupole field is set up, all the ions resulting from the collision of the electrons with the gas atoms present along the path will be expelled by the quadrupole field and are collected by a cylindrical collector screen 10 which surrounds the entire electrode arrangement. The collector screen 10 acts as a shield and is maintained at a negative potential U_s with respect to the cathodes 2 and 3 by means of a battery 11 or other power supply, so that the ions expelled by the field will be collected thereon and a suitable meter, such as an electrometer-type nanoammeter 12, is connected in series with the battery 11 to measure the resulting collector current (i^+).

All the electrodes, with the exception of the cathode 2, may be constructed from non-magnetic stainless steel and mounted

3,665,245

on fixtures of aluminum oxide. The whole electrode structure may be mounted on a stainless steel flanged cap 13 having ceramic feedthroughs 14 for the electrical leads. The cap 13 is attached to the casing 1, which may be in the form of a stainless steel tube and the cap flange 13a may be tightened to the tube with a copper sealing ring (not shown).

QUADRUPOLE FIELD TUNING

In order to determine the proper operational parameters to produce the desired quadrupole focusing of the electrons, we must consider the relation of these parameters to the electric field. We will define the coordinates of the field as shown in FIG. 2, the X-coordinate being the axis of the casing 1 and the Z and Y coordinates passing through the centers of the opposite pairs of rods 6a, 6b and 7a; 7b, respectively. The electric field within the quadrupole electrodes is given by the equations.

$$E = -\text{grad} \left\{ \frac{U_{do} + U_0 \cos \omega t}{r_0^2} (y^2 - z^2) \right\} \quad (1)$$

$$-eE = m \frac{d^2 y}{dt^2} j + m \frac{d^2 z}{dt^2} k \quad (2)$$

where r_0 is the inner radius of the quadrupole arrangement. This leads to the following differential equations for Y and z:

$$\frac{d^2 y}{dt^2} - \frac{2e}{mr_0^2} (U_{do} + U_0 \cos \omega t) y = 0 \quad (3)$$

$$\frac{d^2 z}{dt^2} + \frac{2e}{mr_0^2} (U_{do} - U_0 \cos \omega t) z = 0 \quad (4)$$

Both are of the form of Mathieu's equation:

$$(d^2 \zeta / d\theta^2 + (a - 2q \cos 2\theta) \zeta = 0 \quad (5)$$

the solution of which is given in "Theory and Application of Mathieu Functions", N. W. McLachlan, 1947, Claredon Press, London and New York, as:

$$\zeta = A \exp (\mu\theta) \sum_{-\infty}^{+\infty} c_r \exp (iv\theta)$$

$$+ B \exp (-\mu\theta) \sum_{-\infty}^{+\infty} c_r \exp (-iv\theta) \quad (6)$$

This can applied for ζ being either y or z. In the case of the y coordinate (equation (3))

$$a = a_y = -(8eU_{do}/r_0^2 m w^2) \quad (7)$$

and in the case of the z coordinate (equation (4))

$$a = a_z = +(8eU_{dc}/r_0^2 m w^2) \quad (8)$$

and in both cases

$$q = (4eU_0/r_0^2 m w^2) \quad (9)$$

which results from the fact that the time operator d^2/dt^2 has to be replaced by the operator $(w^2/4) (d^2/d\alpha^{1/2})$, since $\theta = wt/2$. The characteristic exponents μ of the solution can be determined from a and q. But in order that y and z may be real, μ has to be purely imaginary of the form $\mu = (b/d)t$, where b and d are integral numbers. The upper limits for a_z and the lower limits for a_y are given by

$$a_y = -BA^2 U_0^2 \left(1/2 - \frac{7A^2 U_0^2}{128} \right) \quad (10)$$

and

$$a_z = B \left(1 - AU_0 - A^2 U_0^2 + \frac{A^2 U_0^3}{64} - \frac{A^4 U_0^4}{1536} \right) \quad (11)$$

where $A = 1.77 (10r_0v)^{-2}$; $B = 28r_0^2v^2$; r_0 is in meters; v is in MHz, and U_0, a_y and a_z are in volts.

For example, in a gauge using a frequency of $v = 200$ MHz, the ratio of the peak voltage U_0 and the superimposed dc voltage U_{dc} can be determined. For electron focusing when $a_y = a_z$ the ratio U_0/U_{dc} equals 6.05. This means that for a peak voltage of $U_0 = 160$ v, the DC potential should be $U_{dc} = 27$ v. Values of a_y and a_z under these conditions are represented by the two curves in FIG. 3. In these curves a_y and a_z are given in

units of U_0, as a function of the peak voltage U_0 for electron and for a high frequency of $v = 200$ MHz as applied to the. In order, then, that only electrons remain on a stable trajectory, the gauge should be operated at values close to the points of the two curves which yield $a_y = -a_z$. It will be that this is the case approximately at $U_0 = 160$v, which fixes the value for U_{dc} at 27v. For values of $U_0 > 160$v, one still have stable trajectories for electrons, but other charged particles with higher masses M may also become stable. DC potential U_{dc} then to be applied can be determined from the intersection of the line, as given by $U_{dc} = -\gamma U_{o1}$, with lower curve of FIG. 3. γ is smaller than 0.166 and U_{o1} varies between O and U_0. From the corresponding value for U_{o1} can find the range of masses up to which stable conditions exist. All charged particles with atomic weights smaller than

$$A = 5.45 \times 10^{-4} U_0/U_{o1} \quad (1)$$

then fulfill these conditions for a device constructed in accordance with the present invention with $r_0 = 1$ cm and using $v = 200$ MHz. For ions with $A = 1$ (hydrogen), a ratio of $U_0/U_{o1} \cong 1,840$ would be necessary, which shows that with $\gamma < 0.166$ practically only electrons will oscillate under stable conditions. Owing to the long electron path, the number of ions produced will be much higher than in prior ionization gauges.

The device may be tuned for the maximum collector current, which coincides with the theoretical relationship for best electron focusing. however, the electrodynamics will only be valid if electrons are free to move. As soon as the electrons hit a gas atom or molecule, they will deviate from the desired movement. Under ideal conditions the unperturbed electrons will move indefinitely back and forth along the trajectories. The number of unperturbed electrons will increase as the pressure decreases. At pressures of 10^{-13} torr an electron will have a mean free path of approximately 10^{11} cm in dry air. An electron of such a long mean free path will travel back and forth in the tube as long as "8 min" until it suffers a collision which could lead to ionization. Assuming a 10% probability for such an event at a pressure of 10^{-13} torr, ion currents of the order of microamperes can be expected. Calibration measurements conducted with this quadrupole ionization gauge have obtained such high currents at the collector screen.

CALIBRATION

The system used in calibrating the quadrupole ionization gauge is shown in FIG. 4. The system comprises a vacuum chamber 20 having an inlet 21 from the atmosphere controlled by a needle valve 22 and an outlet 23 controlled by a main valve 24. The vacuum was produced with an ion pump 25 connected to the outlet 23 and backed up by a sorption pump 26. The ion pump used was an Ultek Boostivac ion pump commercially obtainable from Perkin-Elmer Corporation, Norwalk, Connecticut. A conventional ionization gauge 27 was connected to the chamber 20 along with the quadrupole ionization gauge 28. The conventional gauge used was a Redhead Ionization Gauge commercially obtainable from National Research Corporation, Cambridge, Massachusetts. The entire system was constructed with stainless steel flanges which were sealed with copper rings and Granville-Phillips type bakeable valves. It was therefore possible to bake the system at 400° C. The quadrupole ionization gauge 28 was calibrated using dry air and argon at room temperatures. Two different procedures were used during calibration. One with a static closed system and the other with a dynamic system where an equilibrium between pumping speed and gas inlet was maintained to establish a certain pressure.

In the first procedure, before calibration, the main valve 24 was closed to disconnect the system from the ion pump 25. The needle valve 22 was then used to let the gases into the system in steps up to a certain pressure. For each step, after stabilizing, the pressure was read on the Redhead Ionization Gauge 27 and the optimum collector current as indicated on meter 12 was noted.

In the other procedure, the system was calibrated by leaving the main valve 24 open and having the needle valve 22 throt-

5

lled until a certain pressure was stabilized due to the continuous pumping of the ion pump 25. Again, a number of pressure points were established and the Redhead Ionization Gauge 27 and the quadrupole gauge meter 12 were read. Various calibration curves were plotted and no noticeable differences were noted between them and those of the former procedure other than a slight spread of the measured points due to the slight pumping action.

IONIZATION GAUGE

In the earliest form of quadrupole ionization gauge tested, the cathode 3 was used as the ion collector electrode. As shown in FIG. 1a, cathode 3a was connected to the negative terminal of a battery 11 a so as to make its potential negative with respect to cathode 2a and the screen 10 was used merely as a shield and grounded along with the positive side of the cathode power supply 18a The quadrupole electrodes and the mode were connected as shown in FIG 1. The gauge constant C for this arrangement as defined by $C_p = i^+/i^-$, that is, the conditions under which the ion current i^+ was proportional to the pressure p and the electron current i^-, was determined before the high frequency generator was set in operation. Under these DC conditions with the quadrupole rods only at potential U_{dc}, the constant did not exceed a value of $C=50$ torr^{-1}. This is a factor of 10 higher than presently used ionization gauges so that this early gauge in DC operation was 10 times as sensitive as the ionization gauges of the prior art

When an alternating field having a frequency $v = 200$ MHz was applied to the quadrupole electrodes, using the operating parameters $U_o = 160$v, $U_{dc} = 27$v, for an optimum collector potential $U_s = -19.5$v a gauge constant having the value $C=10^4$ torr^{-1} was determined Thus, an ionization gauge of an even greater sensitivity was achieved using an RF field

However, even more startling results were obtained with an ionization gauge of the preferred form shown in FIG 1 wherein the shielding screen 10 is used as the ion collector. While in the DC mode of operation, with similar operating parameters, the sensitivity of this gauge (FIG. 1) was equivalent to the earlier model (FIG. 1a) but when the RF voltage with $v = 200$ MHz was applied to the quadrupole electrodes the collector current, as read on meter 12, was found to increase with decreasing pressure within the range from 10^{-8} to 10^{-10} torr according to the relationship $p(i^+)^n = c$

Calibration curves were measured using this gauge (FIG. 1) at different high frequency power inputs and different electron emission currents and are shown in FIGS. 5 and 6. FIG. 5 corresponds to a calibration at an initial electron emission of 100μA and a high frequency power of about 20 watts FIG 6 depicts three calibration curves at three different electron emission currents of 10, 50 and 100μA and a higher high-frequency power input of about 40 watts.

By adjusting the power supply 18 for heating the filament 2, the emission current was set with only the dc potential on the quadrupole rods 6a, 6b, 7a, 7b. Switch 30 in line 31 was then opened and the high frequency voltage was applied. After applying the high frequency with the correct peak potential, the emission current (i^-) as measured at the amperemeter 9 dropped down to between 1 and 10 percent of its initial value. This would seem to indicate that due to electron focusing and oscillation, a negative space charge built up and prevented further electron emission from the cathode 2. A high alternating current existed within the center of the tube 1. The fact that the emission current dropped to such a low value also indicates that very few electrons of high energy struck solid parts within the tube 1.

The exponent n of the equation $p(i^+)^n = c$ was determined for the respective curves, as well as the constant c, and the values are listed in the following table, where p is measured in torr and (i^+) collector current is measured in amperes.

	i-(UA)	n	c
	100	1.30	3.88×10^{-14}
6.2	10	1.31	2.88×10^{-17}
6.1	50	1.33	2.63×10^{-15}
6.3	100	1.29	5.37×10^{-15}

6

As can be seen from FIGS. 5 and 6, the inverse pressure dependence held in the range from 10^{-7} to 10^{-10} torr without any indication that the collector current will decrease with decreasing pressure.

This inverse mode of operation is of extreme advantage for measuring very low pressures since currents in the range of microamperes are being measured. Thus, the insulation problems inherent in most ionization gauges where currents in the order of 10^{-15} amperes and lower have to be measured or amplified are obviated with this gauge. It has been found that collector currents in the order of microamperes can be obtained at pressures as low as 10^{-10} torr with an electron emission of 100 microamperes which corresponds roughly to an ionization yield of 10^7 ions/cm/torr. Such a high ionization yield indicates a high pumping speed in the lower pressure range so that the gauge can be readily adapted for use as an ultra-high vacuum ion pump.

Ion Pump

In the ion pump mode of operation, the cathode 3 of the gauge shown in FIG. 1 is modified to consist of a mesh made of titanium or alternatively a narrow spiral of titanium wire 33, either of which may be heated to produce titanium vapor that can be available for getter action. As shown in FIG. 7, a flat ring 34 is positioned immediately in front of the spiral cathode 33 and set at the same potential.

When the quadrupole optics are properly tuned, the electrons, as in the ionization gauge, will follow a narrow spiral and reach their maximum axial velocity when passing through the anode ring 5 They are then slowed down by the inverted field of the cathode 3 and are given a reverse acceleration thereby. The free electron path will thus be a very long oscillating spiral and will only end its free movement when colliding with a gas atom At very low pressures, for example, 10^{-12} torr, the path may be as much as 1 $^{-10}$ cm

In constructing an ion pump, the operating parameters are again chosen so that only electrons are focused by the quadrupole field. A formula for the frequency of such a field in terms of the maximum voltage U_o of the high frequency generator 8, the internal quadrupole electrode radius r_o, and the mass of the charged particle m is given by the relationship

$$v = 1.03 \times 10^{-6} \frac{1}{r_o} \left(\frac{U_o}{m} \right)^{1/2} \qquad (13)$$

where the frequency is in Hertz when U_o is in volts, r_o is in meters, and m is in kilograms. For an electron, the above formula reduces to

$$v = 1.08 \times 10^5 r_o^{-1} U_o^{1/2} \qquad (14)$$

A suitable maximum voltage U_o for the generator 8 is, for example, 5,000 volts and using an internal electrode radius $r_o = 10$ cm, a frequency of $= 75.5$ MHz, will be required. With such an arrangement, the electrons will stay in the center of the quadrupole while all other charged particles will end up on the walls. The length of the ion pump discharge tube should be made such that the time-of-flight of the electrons is long in comparison to the duration of a higher frequency period From the equations of motion that determine the electron path, the dc potential U_{dc} which must be imposed on the anode ring 5 can be calculated. For optimum electron focusing the ratio between the peak voltage U_o of the high frequency generator 8 and the dc voltage U_{dc} of the anode 5 is given by

$$U_{dc} = 0.17 U_o \qquad (15)$$

this will require a DC voltage of 850 volts to achieve optimum operation with the other parameters given

With this ion pump, a sorption pump may be used as forevacuum pump (in the manner shown in FIG 4) and provisions should be made for very wide fore-vacuum connections at both ends of the tube and at the walls where the ions arrive with velocities up to 850 eV. Since this is, of course, much faster than the thermal motion, in addition to the getter-ion "-pumping" action, a real-ion pumping action will also occur. This is an important feature of the present ion pump

In all known ion pumps now in use, the gas molecules are really not being pumped out of the system but they are rather being absorbed at the walls that are made fit for such a process

by evaporation of getter materials. However, a real pump should be one where the molecules to be pumped will completely leave the system, that is, for example, as shown in FIG. 4, the ionized gas atoms and molecules will leave the pump 25 completely and will be pumped out of the vacuum system by the forepump 26 into the atmosphere. This is possible when the ion flux towards the fore-vacuum is larger than the back streaming of neutral molecules. With the high-ion velocities and greater ion production efficiency obtainable with the present device, it is possible to achieve such a real pumping action. Such a pumping action makes the device especially suitable for noble gas pumping which has always been a problem for getter-ion pumps and in addition the danger of re-emitting the pumped gas is reduced.

If it is desired to increase the efficiency of the present device, several sets of electrodes can be inserted within a single casing parallel to each other and the high frequency power may be transmitted using opposite pairs of rods as the transmission lines. The different sets of electrodes or cells can then be connected in series with each other as shown in FIG. 8, with the negative electrodes 6a–6e and the positive electrodes 7a–7d commonly connected. A single one of these cells (6a, 6b, 7a, 7b) with the above-indicated electrical characteristics has been found to have a pumping speed of at least 15 liters per second so that very high pumping speeds are obtainable with the arrangement of the present invention.

A nonmagnetic ionization gauge is thus presented which is many orders of magnitude more sensitive than the gauges of the prior art and which may be operated in such manner as to obtain a calibrated current in inverse relationship to the measured pressure within the pressure range from 10^{-8} to 10^{-10} torr, and below, and which in an enlarged version may be adapted to operate as an ion pump capable of pumping speeds far beyond those obtainable with existing ion pumps. The device achieves strong focusing of electrons using only electric fields thus obviating the need for any magnetic components.

I claim:

1. A non-magnetic ionization device comprising.
    a. means for producing an oscillating stream of electrons,
    b. means for producing an electric field for focusing and confining said stream in continuous oscillation within a substantially restricted path and for expelling from said path ions resulting from the collision of said electrons with atoms in said path, and
    c. means disposed about said field-producing means for collecting the ions expelled from said path

2. A device as in claim 1 wherein said electric field-producing means comprises a set of quadrupole electrodes

3. A device as in claim 1, wherein said stream-producing means comprises spaced cathodes, and an anode disposed between and at a positive potential relative to said cathodes and wherein said electric field-producing means comprises quadrupole electrodes arranged about an axis defined by said stream and at substantially the same potential as said anode.

4. A device as in claim 3 wherein said quadrupole electrodes are supplied with a high frequency voltage $U_o\cos\omega t$ for creating an electric field whose respective components along the Y and Z axes through the opposite pairs of electrodes are of the form

$$\frac{d^2y}{d\theta^2}+(a_y-2q\cos 2\theta)y=0$$

$$\frac{d^2z}{d\theta^2}+(a_z-2q\cos 2\theta)z=0$$

$$a_y=-\frac{8eU_{do}}{r_0^2m\omega^2}$$

$$a_x=+\frac{8eU_{do}}{r_0^2m\omega^2}$$

$$q=\frac{4eU_0}{r_0^2m\omega^2}$$

U_o being the anode voltage, r_o being the inner radius of the quadrupole electrodes, e/m being the charge to mass ratio of an electron and

$$a_y\geq BA^2U_o^2\left(1/2-\frac{7a^2U_o^2}{128}\right)$$

$$a_x\leq B\left(1-AU_0-A^2U_0^2+\frac{A^2U_0^2}{64}-\frac{A^4U_0^4}{1536}\right)$$

where $A=1.77\,(10r_o\nu)^{-2}$, $B=28\,r_o^2\nu^2$; r_o is in meters; ν is the operating frequency in MHz, and U_o, a_y and a_x are in volts

5. A device as in claim 3 wherein said ion collecting means comprises one of said cathodes at a negative potential relative to the other cathode

6. A device as in claim 3 wherein said ion collecting means comprises an annular electrode disposed about said quadrupole electrodes and at a negative potential relative thereto

7. A device as in claim 3 wherein one of said cathodes comprises a metallic electrode heated to produce a vapor for getter action.

8. An ionization gauge comprising:
    a. two spaced electrodes,
    b. a third electrode disposed between said spaced electrodes and at a positive potential relative to each and having an opening therein to permit a stream of electrons to follow an oscillating path between said spaced electrodes for ionizing atoms in said path,
wherein the improvement comprises:
    c. quadrupole electrode means disposed about said path at approximately the same potential as said third electrode and having a high frequency voltage impressed thereon for confining said electron stream within said path and expelling ions resulting from the ionization of atoms in said path; and
    d. a cylindrical electrode surrounding said quadrupole electrode means and at a negative potential relative thereto for collecting the ions expelled from said path.

9. An ion pump comprising.
    a. a first heated cathode for emitting a supply of electrons;
    b. a second heated cathode for producing a vapor for getter-ing action,
    c. an anode disposed between said first and second cathodes and at a positive potential relative to each,
    d. a set of quadrupole electrodes disposed about an axis defined by said cathodes and said anode and at substantially the same potential as said anode and having a high frequency voltage impressed thereon for setting up an electric field tending to focus said supply of electrons along a confined oscillating path and to expel any ions in said path, and
    e. means for collecting said expelled ions.

10. An ion pump as in claim 10, wherein the high frequency voltage has a frequency of $1.08\times10^5r_o^{-1}U_o^{1/2}$ Hertz r_o being the internal quadrupole electrode radius in meters and U_o being the maximum voltage in volts.

*　*　*　*　*

Exhibit 5

Proceedings
of the
Sixth International Vacuum
Congress

March 25-29, 1974
Kyoto International Conference Hall
Kyoto, Japan

Theory of the Quadrupole Ion Pump*

Heinrich Hora** and Helmut Schwarz

Rensselaer Polytechnic Institute Hartford, Connecticut 06120 USA

The high pumping speed of the quadrupole ion pump for pressures down to 10^{-10} Torr is due to the long interaction time of the electrons confined by the HF field. A theory for the residual ion current i_0^+ being proportional to $p^{-0.7}$ (i.e., i_0^+ almost inversely proportional to the pressure p) is based on the generation of a plasma along the axis of the quadrupole. Since the orbits of the electrons are centered at the axis only-in contrast to magnetic confinement (Penning Gauge)-the plasma volume depends strongly on the collisions of the electrons described by stable solutions of Mathieu's differential equations We derived the measured relationship for i^+ and arrived at electron densities to be 10^{10} cm^{-3} at pressures of the order of 10^{-10} Torr.

§1. Introduction

In the quadrupole ion pump[1-3] electrons are electrodynamically confined axially to stable trajectories by an RF quadrupole field and trapped lengthwise by the cathode and anti-cathode. The consequent ionization of gas molecules results in a removable ion current. The remarkable property of the quadrupole system consists in an increase of the ion current i^+ while decreasing the pressure[2] p. Such an unusual inverse relationship between ion current and pressure had been observed independently by E. W. Blauth[4] who, however, did not investigate the phenomenon further. The relationship

$$i^+ \propto p^{-0.7 \pm 0.1} \qquad (1)$$

was derived from measurements indicating a favorable use of the system as an ionization gauge for pressures between 10^{-5} and 10^{-11} Torr.

During pumping, the exponent of Eq. (1) became smaller due to the well known re-emission of the "pumped" gases. Speeds of a few hundred liters/sec at 10^{-9} Torr were achieved.[3]

The theory of the initial ion current of the quadrupole pump is based on a confinement of the electrons by the electrodynamic field of the system, where ions are electrostatically enclosed to create a stationary plasma. The analogy to the Penning ion pump consists in the movement of electrons on stable orbits. While the magnetic confinement in the Penning pump permits orbits at any center, the centers of the electron orbits in the quadrupole coincide always with the axis of the system.

§2. The Quadrupole Systems and the Generated Plasma

As described before,[1-3] the quadrupole pump consists of four parallel electrodes of spherical or hyperbolic cross sections (see Figs. 1 and 3 of Ref. 1, Fig. 1 of Ref. 2, and Fig. 1 of this paper). They are symmetrically charged by an RF voltage of a peak value U_0 and frequency ω superimposep by a dc potential U_{dc}. The electrodes carry a potential U:

$$U = U_{dc} + U_0 \cos \omega t \qquad (2)$$

At one end of the cylindrical structure is a thermionic electron source and, at the other end, a flat spiral on the same potential, see Figs. 1 and 2. In the middle is a ring having the dc
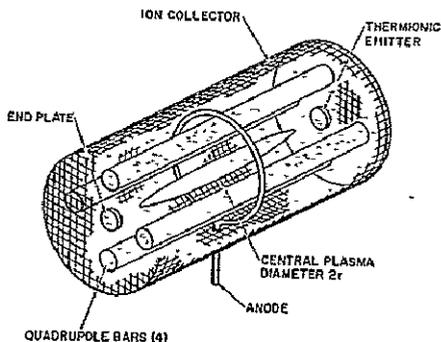
Fig. 1. Schematics of quadrupole ion pump and quadrupole ion gauge with a stationary central plasma of radius r, in which electrons are confined electrodynamically by an RF field.
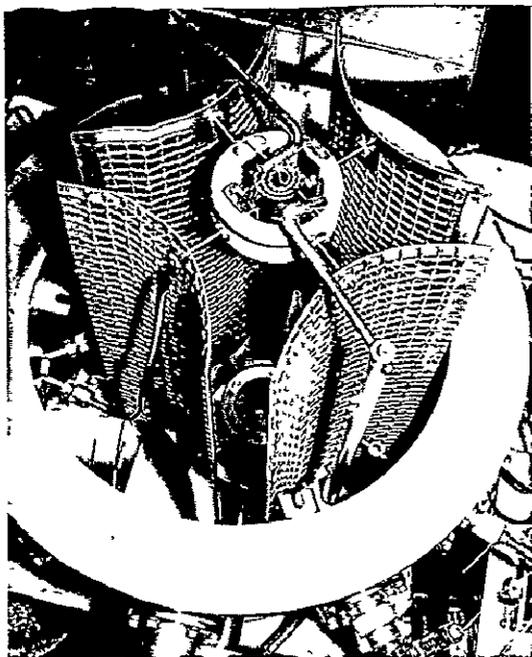
Fig. 2. Photograph of quadrupole ion pump with hyperbolically shaped electrodes of stainless-steel wire mesh; axis is vertical; at bottom there is a hair pin filament for electron emitter and at top a tantalum spiral covered with titanium serving as anti-cathode as well as supplier for getter.

potential U_{dc}; it collects the electron current i^-. Everything is surrounded by a cylindrical screen or tube which is on a negative potential U_{screen} collecting the ion current i^+.

U_0, U_{dc} and ω are selected according to solutions of Mathieu's differential equation so that the electrons move on stable trajectories.[1-3,5] Wuerker et al.[6,7] observed these trajectories by injecting charged small powder particles. Similar processes of electrodynamically orbiting electrons are related to dynamic stabilization of a plasma.[8]

For an optimum operation of an ion gauge, the RF had to be 200 MHz, with $U_0=165$ volts, while U_{dc} had to be 27 volts.[1,2]

Our theory is based on the following model. After passing through a certain initial transition period, an unusual kind of plasma is created in the center of the quadrupole along the axis. Electrons oscillating between the ends are kept in stable Mathieu-kind trajectories. This motion is disturbed only by collisions with electrons, ions, and neutrals. At higher pressure a central plasma of small diameter will result, while at lower pressures the central plasma increases. In a larger plasma, more

electron-ion pairs will be created, being detected as currents i^- and i^+, which explains the observations by eq. (1).

§3. Detailed Formulation of Theory

We can express the number of ions, i^+, collected at the screen by:

$$i^+ = i_{gen} - i_{recomb} \qquad (3)$$

Here i_{gen} describes the rate of all ions created in the system and i_{recomb} the rate of ions lost by recombination.

3.1 Ions generated

i_{gen} can be calculated from the following sum of integrals:

$$\begin{aligned}
i_{gen} = &\iiint_{V_{plasma}} dx dy dz \sigma_e^i(\langle \varepsilon_e \rangle, \langle T_n \rangle) n_n n_e \\
&+ \iiint_{V_{plasma}} dx dy dz \sigma_i^i(\langle \varepsilon_i \rangle, \langle T_n \rangle) n_n n_i \\
&+ \iiint_{V_{rest}} dx dy dz \sigma_e^i(\langle \varepsilon_e \rangle, \langle T_n \rangle) n_n n_e \quad (4)\\
&+ \iiint_{V_{rest}} dx dy dz \sigma_i^i(\langle \varepsilon_i \rangle, \langle T_n \rangle) n_n n_i \\
&+ W_{gen}
\end{aligned}$$

Hereby, the first integral taken over the plasma volume (V_{plasma}) gives the rate of ion-pair production due to the impact of electrons with neutrals; the second due to impact of ions with neutrals. Correspondingly, the third and fourth integrals give the ion-pair production due to the impact of electrons or ions respectively with neutrals within the "rest volume" (V_{rest}), i.e. total volume of quadrupole tube minus volume of plasma (V_{plasma}). σ_e^i, σ_i^i are the rate densities for the ion-pair productions. They depend on the electron energy ε_e and ion energy ε_i respectively. Both depend, of course, on the temperature T_n of the neutrals. n_e, n_i, and n_n are the densities of the electrons, ions and neutrals.

The influence of attachment and detachment processes can be neglected, because no negative ions will reach the screen to influence i^+ and because the neutrals created by detachment will be included in the expressions for n_n. The fifth term in eq. (4), viz, W_{gen} is the ion creation due to interaction of ions or photons with the wall.

3.2 Ion losses

The deficit of ions (i_{recomb} of eq. (3)) due to recombination processes can be described in

analogy to eq. (4). However, in first approximation all recombination processes can be neglected as pointed out in the evaluation below.

3.3 Evaluation

In order to obtain a first insight into the mechanisms, we neglect the following processes:

1) Recombination at the wall, W_{recomb}

2) All processes occurring in the rest volume, V_{rest}

3) All recombination processes

4) Ionization by ions

These omissions are justified, since we are dealing with very low pressures. W_{recomb} will contribute less than 10% due to the geometry of the electrodes causing a kind of shadow modified by the electrostatic and the alternating electric fields.

W_{rest} can be omitted, since there are very few electrons outside the plasma. Also the neutrals will have a much lower density than the electrons which allows to neglect all ion creation processes in V_{rest}.

As to the third process, recombinations, it seems reasonable to neglect these also, considering the dimensions of the apparatus.

However, ionization by ions inside and outside of the plasma may be of concern. This depends on the ability of the ions, especially those of the actual plasma, to gain the necessary energy from the stable oscillating electrons. If the ions, after being created in the plasma, leave with their primary thermal energy, then they cannot produce pairs before having been accelerated by the dc-voltage of the screen. However, further experimental information, especially on the ion energy within the central plasma are needed. The assumptions lead to results which agree well with the experiments. Evaluating the equations (3) and (4) leads to:

$$i^+ \simeq \iiint_{V_{plasma}} dx\,dy\,dz \frac{1}{\varepsilon_{e2}-\varepsilon_{e1}}$$
$$\times \left[\int_{\varepsilon_{e1}}^{\varepsilon_{e2}} \frac{s_e(\varepsilon_e,\,T_n)}{n_{00}} v_e(\varepsilon_e)n_e(\varepsilon_e)d\varepsilon \right] n_0(x,\,y,\,z) \tag{5}$$

Where ε_{e1} and ε_{e2} are the limits of the actual electron energies which generally depend on x, y, and z. v_e is the velocity of the electrons. s_e is the ionization efficiency[10] for one electron of an energy ε_e given by the number of pairs created per cm in gases of 0 °C temperature and

of 1 Torr pressure. For electron energies ε_e smaller than the double value of the ionization energy ε_{i0} ($\varepsilon_e \leq 2\varepsilon_{i0}$):[11]

$$s_e(\varepsilon_e)=a(\varepsilon_e-\varepsilon_{i0}) \tag{6}$$

The constant a can be taken from Table 2.1 of ref. 11 and is for nitrogen: $a=0.26$, if ε_e and ε_{i0} are given in volts. n_{00} is the neutral particle density at 1 Torr and 0°C. $n_0(x,\,y,\,z)$ is the actual particle density at the existing pressure p.

Entering with eq. (6) into eq. (5) and assuming that n_e is independent and that the plasma-volume-integration leads to an average value for $n_0 V_{plasma}$, we arrive at the following integral taken over the electron energies:

$$i^+ = 10^2 n_e n_0 V_{plasma} \frac{a(2em^{-1})^{1/2}}{n_{00}(\varepsilon_{e2}-\varepsilon_{e1})}$$
$$\times \int_{\varepsilon_{e1}}^{\varepsilon_{e2}} (\varepsilon_e-\varepsilon_{i0})\varepsilon_e^{1/2}d\varepsilon_e \tag{7}$$

(e-elementary charge in Coulomb; m-electron mass in kg)

Evaluating the integral in eq. (7) and contracting all constants in one constant:

$$A_0 = 10^2 a n_e p V_{plasma}(2em^{-1})^{1/2} \tag{8}$$

(where $p=n_0/n_{00}$ as per definition of n_0 and n_{00}) one arrives at:

$$i^+ = \frac{A_0}{\varepsilon_{e1}^{1/2}+\varepsilon_{e2}^{1/2}} \left[\frac{2}{5}\{\varepsilon_{e1}^2 + (\varepsilon_{e1}^3\varepsilon_{e2})^{1/2}+\varepsilon_{e1}\varepsilon_{e2} \right.$$
$$+(\varepsilon_{e1}\varepsilon_{e2}^3)^{1/2}+\varepsilon_{e2}^2\}$$
$$\left. -\frac{2}{3}\varepsilon_{i0}(\varepsilon_{e1}+\varepsilon_{e1}^{1/2}\varepsilon_{e2}^{1/2}+\varepsilon_{e2}) \right] \tag{9}$$

By introducing the average electron enrgy $\bar{\varepsilon}_e$ and taking into account that the lower limit ε_{e1} is mostly much smaller than the upper limit ε_{e2}, Eq. (9) can be transformed to the approximation:

$$i^+ \propto \bar{\varepsilon}_e^{+3/2} \tag{10}$$

The assumption that n_e is independent of the size of the plasma is justified by the fact that the electron concentration is mainly a question of the Mathieu trajectories of the electrons. The length of the plasma (assuming to have the shape of an ellipsoid, see Fig. 1) is constant; therefore it changes only its diameter so that V is proportional to r^2, whereas n_0 is inversely proportional to r^2 turning the product $n_0 V$ into a constant. The average electron energy itself

should be, in first approximation, proportional to that linear dimension of the plasma which changes, namely r.

$$\bar{\varepsilon}_e \propto r \tag{11}$$

At present, we have no detailed information on the disturbances of stable orbiting electrons by collisions, but we may assume that the linear dimension r is related to the pressure p by:

$$r \propto p^{-1/2} \tag{12}$$

Equation (10) can now be written as:

$$i^+ \simeq A_0 \bar{\varepsilon}_e^{+3/2} \propto p^{-3/4} \tag{13}$$

This is in agreement with the measured relationship, eq. (1).

The assumed r-p-dependence, eq. (12), fits the necessary condition that a variation of p by nearly four orders of magnitude should allow the variation of r by a factor of one hundred; this certainly lies within the dimensions of the apparatus.

The theory also yields reasonable values for the electron density n_e of the central plasma. Equation (10) and the value of A_0 (eq. (8)) lead to the electron density:

$$n_e \simeq \frac{i^+ m^{1/2}}{p V_{\text{plasma}} a (2e)^{1/2+(3/2)} \bar{\varepsilon}_e} 10^{-2} \tag{14}$$

Entering into (14) with a pair of values for $i^+ = 6 \times 10^{-5}$ amp and $p = 1.5 \times 10^{-9}$ Torr as measured in ref. 2 (see Fig. 3 of ref. 2) and assuming a plasma volume $V_{\text{plasma}} = 1000$ cm^3 and an average electron energy of $\bar{\varepsilon}_e = 100$ volt will render an electron density of

$$n_e \simeq 1.6 \times 10^{10} \text{ cm}^{-3}$$

This is quite a reasonable value. The cut-off density of the plasma for the applied 200 MHz RF-field is lower than n_e and does not have an effect because the dimensions of the plasma are very much smaller than the skindepth of this wave length.

It is worthwhile to mention that such a quadrupole-stabilized plasma opens interesting aspects for plasma physics because the ions are only electrostatically trapped by the electrons.

References

1) H. Schwarz: *Proc. 4th Intern. Vac. Cong., Manchester, England, 1968*, p. 685
2) H. Schwarz and H. A. Tourtellotte: J. Vac Sci. Technol. 6 (1969) 260.
3) H. Schwarz: J. Vac. Sci. Technol 9 (1972) 373
4) E. W. Blauth: Private communication to one of the authors (H. Schwarz) at the 4th Intern Vac Congress, Manchester, England. April 1968.
5) W. Paul and M. Raether: Z. Physik 140 (1955) 262.
6) R. F. Wuerker, H. Shelton and R. V. Langmuir: J. Appl. Phys. 30 (1959) 342.
7) R. F. Wuerker, H. M. Goldenberg and R. V. Langmuir: J. Appl. Phys. 30 (1959) 441.
8) H. P. Furth and J. B. Taylor: Bull. Am. Phys. Soc. 14 (1969) 1029.
9) E. Hinnov and J. G. Hirschberg: Phys. Rev. 125 (1962) 795.
10) A. von Engel: *Ionized Gases* (Clarendon Press, Oxford, England 1965) 2nd Ed , p. 63.
11) G. Francis: *Ionization Phenomena in Gases* (Butterworths Scientific Publications, London, 1960) p. 26.

Exhibit 4

Quadrupole Ion Pump Performance Characteristics *

Helmut Schwarz

Rensselaer Polytechnic Institute, Hartford, Connecticut 06120
(Received 28 July 1971)

The new nonmagnetic ion pump resembles the quadrupole ionization gauge. The dimensions are larger, and hyperbolically shaped electrodes replace the four rods Their surfaces follow $y^2 = 36 + x^2$ (x, y in centimeters). The electrodes, 55 cm long, are positioned lengthwise in a tube At one end a cathode emits electrons; at the other end a narrowly wound flat spiral of tungsten clad with titanium on cathode potential can be heated for titanium evaporation. Electrons accelerated by a dc potential of the surface electrodes oscillate between the ends on rotational trajectories, if a high frequency potential superimposed on the dc potential is properly adjusted. Pumping speeds (4–100 liters/sec) for different gases at different peak voltages (1000–3000 V) at corresponding frequencies (57–100 MHz), and at different pressures (10^{-5}–10^{-9} Torr) are reported.

Introduction

The operation of the Quadrupole Ion Pump is similar to the Penning type ion pump but has one major difference: It does not use a magnetic field, the confinement of the oscillating electrons being achieved with a quadrupole arrangement tuned for electrons. It is similar to the quadrupole ionization gauge operation.[1,2] Electrons are emitted from a hot hairpin filament at one end and accelerated by a dc potential U_{dc} at the quadrupole electrodes. At the other end of the tube a flat spiral carries the same potential as the cathode causing the electrons to return. Hereby a back and forth movement of the electrons is achieved. A rotational high frequency potential properly adjusted according to the rf quadrupole theory[1,2] keeps the electrons within the center part of the tube volume until they hit a gas molecule. Thus, a very high ionization yield is obtained. The ions will leave the tube volume radially and along the axis, and as in a normal ion pump will be "pumped."

I. Description of Quadrupole Ion Pump

A. Dimensions

The electrodes are mounted in a stainless steel tube. The surfaces of the four quadrupole electrodes are hyperbolic and follow the equation

$$y^2 = 36 + x^2 \quad (x \text{ and } y \text{ given in cm}). \tag{1}$$

The electrode surfaces were cut off at a radius $R = 11.5$ cm. The total length of the electrodes is 55.0 cm. The four hyperbolic surfaces are exactly separated by two ceramic rings at the top and at the bottom. At the top

a tungsten spiral serves as anti-cathode; it is covered with titanium which serves two purposes: (1) to act as the anticathode, and (2) to provide titanium vapor for gettering purposes.

B. Electrical Characteristics

The potentials and frequencies applied to the electrodes are listed in Table I as calculated from the rf excited quadrupole theory for electrons.[1,2] The electron emission current was adjusted to a stable value i^- with only the dc potential U_{dc} applied to the four hyperbolic surface electrodes. After switching on the high frequency potential with peak potential U_0 the emission current i^- decreased to 10% of the initial value.

In operation the quadrupole electrodes carry a potential
$$U = U_{dc} + U_0 \cos 2\pi f t. \tag{2}$$

With the cathode and anticathode at a slightly higher positive potential than ground, an ion current i^+ could be measured at the stainless steel housing. The initial electron emission current i^- was usually adjusted to a value of $i^- = 50$ mA.

C. Fore Pump

As fore pump, two Varian type sorption pumps were applied. Pumping action started at a fore pressure of approximately 10^{-2} Torr.

TABLE I. Potentials and frequencies applied to quadrupole ion pump.

$U_{0[volt]}$	$f_{[MHz]}$	$U_{dc[volt]}$
1000	56.8	170
1800	76.3	306
2400	88.0	408
3000	98.4	510
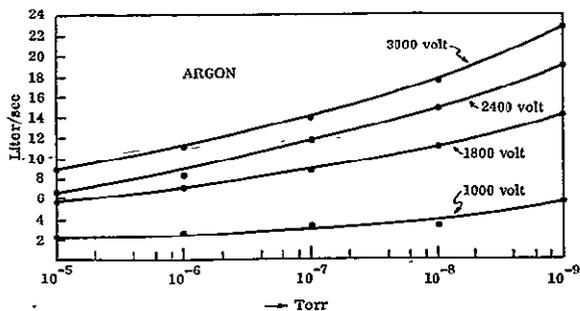
FIGURE 1. Pumping speed as a function of pressure at different peak voltages for argon. $i^- = 50$ mA.

II. Performance of Quadrupole Ion Pump

A. Pumping Speed

A family of curves depicting pumping speeds at different peak voltages with corresponding frequencies and for the different gases is traced on Figs. 1–3. One can see that the pumping speed increases slightly with decreasing pressure but more strongly with increasing peak voltage.

For a given gas and fixed pump characteristic (electron emission i^-, peak voltage U_0, frequency f), the pumping speed as a function of pressure seems to follow a relationship similar to the pressure–collection current dependence of the Quadrupole Ionization Gauge.[2] Such a relationship is possible to express in the following equation

$$p^m S = a. \tag{3}$$

The measurements suggest a value of $m = 0.1$ which holds for all data; however, the constant a depends on the kind of gas and electrical characteristics (peak voltage U_0, frequency f, ion current i^+, etc.).

A more detailed analysis of the measurements of ion current i^+ at different pressures p and varying electrical characteristics leads to the simple relationship:

$$pS = k(i^+ - i_0^+), \tag{4}$$

whereby i_0^+, residual ion current at zero pumping speed, follows the quadrupole ion gauge formula

$$p(i_0^+)^n = c \tag{5}$$

TABLE II. Ionization constants for different gases to be applied in Eq. (14).

Gas	k/k_{air}	k[Torr liter sec^{-1} amp^{-1}]
Dry air	1.00	8.35×10^{-1}
Nitrogen	1.00	8.35×10^{-1}
Argon	1.13	9.43×10^{-1}
Neon	0.22	1.84×10^{-2}
Hydrogen	0.44	3.67×10^{-1}

as established previously.[2] The constant k in Eq. (4) depends solely on the kind of gas used; it has been determined for five different gases—dry air, nitrogen, argon, neon, and hydrogen—and can be taken from Table II. The constant[2] $n = \frac{4}{5}$ in Eq. (5) is independent of the kind of gas; however, c of Eq. (5) behaves similar to the constant a of Eq. (3).

The measurements follow the equations quite well but the physical meaning of the mathematical formulation requires more study of the mechanism.

B. Ultimate Pressure

The lowest pressure so far achieved lies in the range of $10^{-9} \cdots 10^{-10}$ Torr, which seems to be determined by the vapor pressure of some organic sealing materials used in the experimental setup. The pump appears to be capable of reaching lower pressures.

Work is in progress to obtain lower ultimate pressures.

C. "Electronic" Pumping

All existing ion pumps are not "true" pumps in the sense that the gas molecules to be pumped are transported out of the vacuum system into the atmosphere; rather they remain in the pump as buried, adsorbed,

FIGURE 2. Pumping speed as a function of pressure at different peak voltages for hydrogen. $i^- = 50$ mA.
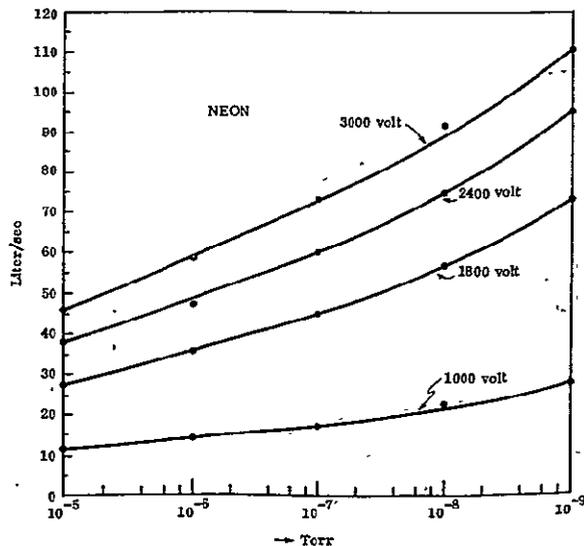
FIGURE 3. Pumping speed as a function of pressure at different peak voltages for neon. $i^- = 50$ mA.

absorbed or even chemically bound on the walls or other solid surfaces of the pump. Therefore, there is always the danger of re-emission of the "pumped" gases. This disadvantage was also observed in the early years of ion "pumps," see for example Ref. 3.

"Electronic" pumping[4–6] for all gases should be more or less equally effective since it depends mainly on the ionization probability and not on gas capture characteristics of the walls and getter materials, which is a great advantage over the conventional ion pumps which "pump" inert gases much less effectively than all other gases. Some attempts[4–6] have been made to achieve "electronic pumping"; however, due to the high rate of return gas flow from the fore vacuum to the high vacuum, the electronic pumping action was quite weak. Since then, little attention[7] has been paid to this kind of ion pumping.

If the hyperbolically shaped electrodes of the quadrupole ion pump are made of wire mesh, the "true pumping" action looks rather promising. The ionized gas molecules achieve a relatively high radial velocity and through appropriate openings they will then enter the fore vacuum. Also their number is relatively high; ion currents in the order of microamperes were obtained at pressures as low as 10^{-9} Torr.

Acknowledgments

References

1. H. Schwarz, Proc. 4th Intern. Vac. Cong., Manchester, England, 1968, p. 685.
2. H. Schwarz and H. A. Tourtellotte, J. Vac Sci. Technol. 6, 260 (1969).
3. H. Schwarz, Z Physik 117, 23 (1940); 122, 437 (1944).
4. H. Schwarz, Symposium on "New Research Techniques in Physics", Rio de Janeiro and S. Paulo, Brazil, July 15–29 (1952), Trans. pp. 405–410.
5. H. Schwarz, Le Vide 42, 1262 (1952); Rev Sci. Instrum. 24, 371 (1953); Errata 25, 924 (1954).
6. J. S. Foster, Jr., E. O. Lawrence, and E. J. Lofgren, Rev. Sci. Instrum. 24, 388 (1953).
7. P. A. Redhead, J. P. Hobson, and E. V. Kornelsen, Advan. Electron. Electron Phys. 17, 382 (1962).